Stockholm University

Bachelor Thesis

Degree Project in
Earth Science 30 hp

A record of deep continental subduction: petrological investigation of the Serre Unit (Dora-Maira Massif, Western Alps)

Miriam A. Wehrli

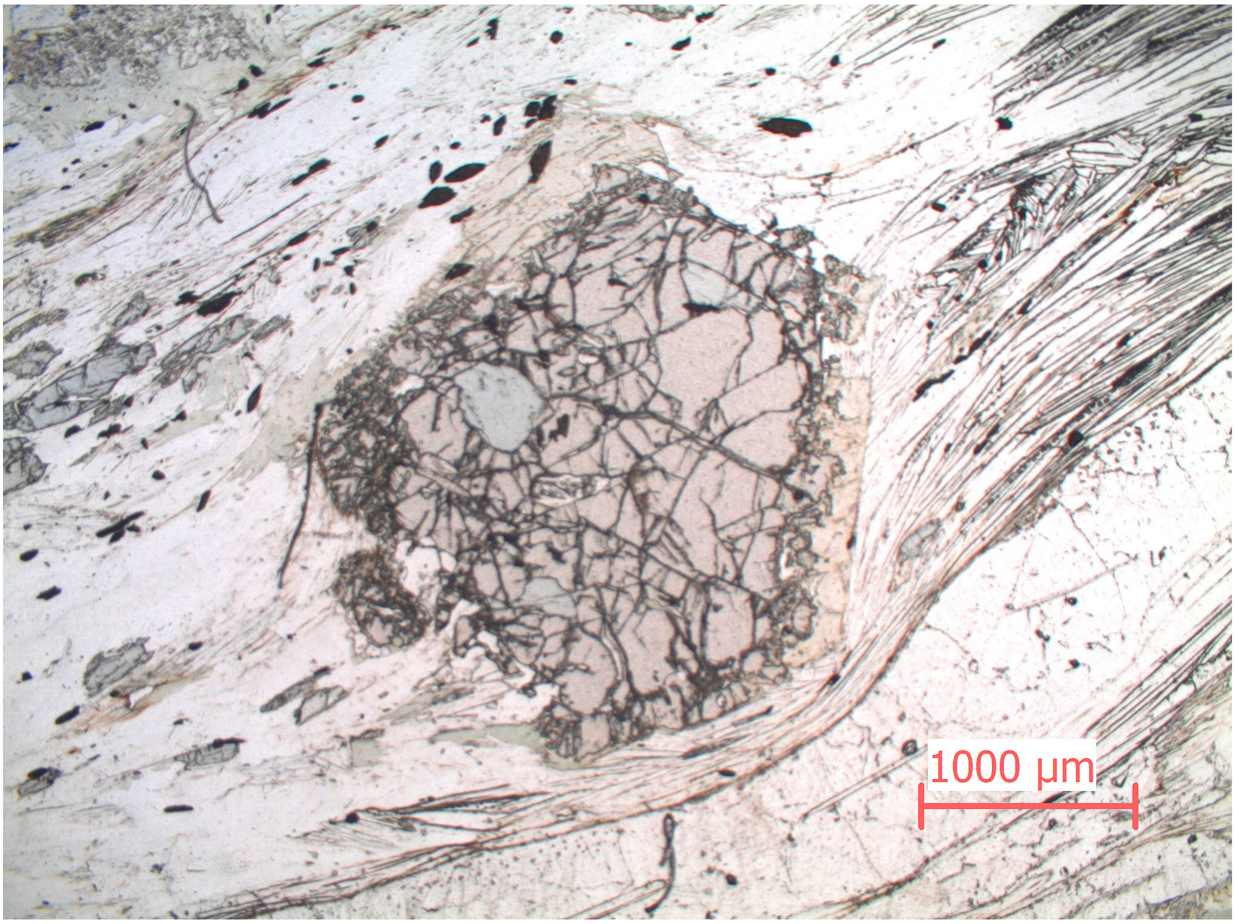

Stockholm 2025

Department of Geological Sciences
Stockholm University
SE-106 91 Stockholm

A record of deep continental subduction: petrological investigation of the Serre Unit (Dora-Maira Massif, Western Alps)

Abstract

The Western Alps represent a collisional orogenic wedge where both ocean- and continent-derived tectonic units are exposed. Here, metamorphic rocks which formed at high- to ultra-high-pressure, low-temperature conditions during continental subduction are exceptionally well preserved. As part of the Western Alps, the Dora-Maira Massif constitutes an excellent site to study the burial and exhumation of (ultra-)high-pressure continental [(U)HP] crustal rocks involved in a subduction zone. Currently, little is known about the metamorphic history and structural architecture of the northern Dora-Maira Massif. From bottom to top, the nappe stack consists of the Pinerolo, Chasteiran, Muret and Serre Units. Recent studies suggest that the Serre Unit has undergone deep subduction during the Alpine orogeny (Manzotti et al., 2022; Nosenzo et al., 2024). However, no *P-T* estimates have been done yet and its precise tectonic history remains unknown. This project investigated the tectonometamorphic evolution of the Serre Unit based on a petrographic analysis of 10 samples. As a result, peak *P-T* conditions for the Serre Unit were estimated equivalent to eclogite facies conditions at 18-23 kbar and 520-580 °C. The stable mineral assemblage at peak metamorphism consists of quartz, white mica, garnet, chloritoid, glaucophane and rutile. The main foliation preserved in the studied samples probably developed after burial during exhumation. Exhumation and cooling are recorded by partial retrogression at greenschist-facies conditions and are associated with brittle deformation and fluid infiltration. These results suggest that the Mesozoic cover rocks of the Serre Unit were indeed involved in deep Alpine subduction similar to the Dora-Maira basement units. Future analysis of the chemical composition of the studied samples as well as calculations of *P-T* pseudosections are needed to either confirm or discard the *P-T* conditions of the Serre Unit inferred in this thesis.

Table of contents

1. Introduction

The Alps of south-central Europe record convergent plate movements during which the European plate was subducted under the Adriatic plate. This tectonic event not only caused the closure of ancient ocean basins but also subsequent accretion and collision processes (Schmid et al., 2022). Consequently, the European Alps represent a collisional orogenic wedge where both ocean- and continent-derived tectonic units are exposed.

The Western Alps run in a north-south direction, forming a tight arc around the western end of the Po Basin. Here, the metamorphic rocks which formed at high- to ultra-high-pressure, low-temperature conditions during subduction of the Briançonnais microcontinent are exceptionally well preserved (Tajčmanová et al., 2021; Bonnet et al., 2022).

The Dora-Maira Massif in the Western Alps is part of the so-called Internal Crystalline Massifs. It is located in the Germanasca valley in northern Italy and stretches for ~70 km from the Susa Valley in the north to the Maira Valley in the south. In the Mesozoic, the Dora-Maira Massif belonged to the distal palaeomargin of the Briançonnais microcontinent facing the Piemonte-Liguria Ocean. Today, it consists mainly of tectonic slivers of Palaeozoic basement and minor remnants of dismembered Mesozoic covers (Manzotti et al., 2022; Nosenzo et al., 2024) which record different pressure-temperature (*P-T)* conditions (Bonnet et al., 2022). Since it was formed by deep continental subduction and the reworking of pre-existing crust, the Dora-Maira Massif constitutes an excellent site to study the burial and exhumation of (ultra-)high-pressure continental [(U)HP] crustal rocks involved in a subduction zone. Indeed, coesite inclusions in garnet crystals found in pyrope-quartzite rocks already indicated ultra-high pressure metamorphism of continental crust in the Dora-Maira Massif in the 1980s (Chopin 1984).

Since then, the internal structure and geometry of the southern Dora Maira Massif has been comparatively well researched, and several tectonic units have been identified on the basis of petrological, lithological and structural observations. They are separated by thrust sheets as well as slivers of ophiolites and Mesozoic meta-sediments. Peak metamorphism reached ranges from garnet-blueschist to quartz-eclogite to coesite-eclogite facies. Moreover, Alpine peak *P-T* conditions for the lowermost unit have been estimated at 14–16 kbar and 400–500 °C or 20–23 kbar and 500–515 °C (Manzotti et al., 2022).

Comparatively little is known about the metamorphic history and structural architecture of the northern Dora-Maira Massif. From bottom to top, the nappe stack currently consists of the Pinerolo, Chasteiran, Muret and Serre Units. The structurally deepest unit (Pinerolo Unit) records Upper Carboniferous graphite-rich metasediments which were intruded by Permian granites and diorites, but no *P-T* estimates have been done yet. The Chasteiran unit has been identified as a cold ultrahigh-pressure metamorphism (UHP) unit with peak *P-T* conditions at 27-28 kbar, 510-530 °C (Manzotti et al., 2022) while thermodynamic modelling for the Muret Unit indicated peak *P-T* conditions of up to 21-22 kbar and 530-560 °C (Nosenzo et al., 2022; Nosenzo et al., 2023).

The recently identified Serre Unit crops out discontinuously in the northern Dora-Maira Massif, on top of the tectonic stack. It consists of Permian-age plutonic, volcanic and volcano-clastic rocks together with remnants of a dismembered Mesozoic cover (Manzotti et al., 2022; Nosenzo et al., 2024). Preliminary observations suggest that this unit includes several different lithologies which form tectonically juxtaposed lenses and discontinuous layers of variable size. Furthermore, its tectonic structure indicates that it is separated at its footwall by a narrow shear zone, the ductile to brittle La Fracho Shear Zone (Nosenzo et al., 2024). It has been suggested that the Serre Unit has undergone deep subduction during the Alpine orogeny as well, but no *P-T* estimates have been done yet and its precise tectonic history remains unknown (Manzotti et al., 2022; Nosenzo et al., 2024).

This project contributes to the investigation of the tectonometamorphic evolution of the Serre Unit which represents the Mesozoic cover of the northern Dora-Maira Massif. Cover sediments are usually sheared off in the processes of continental collision and mountain building and remain stuck near the surface (Pfiffner 2014). Therefore, the study of the Serre Unit provides a rare chance to investigate the tectonometamorphic evolution of a Mesozoic cover nappe that was involved in the process of Alpine subduction. The primary focus of this project is on petrography and the identification of metamorphic reactions, rather than structural investigations. Petrographic analysis and comparisons with peak metamorphic mineral assemblages and corresponding *P-T* conditions of different closely related units from the northern Dora-Maira Massif will be used to estimate peak *P-T* conditions reached during the Alpine orogeny. Based on these results, a hypothesis about the Alpine *P-T* evolution of the Serre Unit will be proposed.

2. Geological Setting

Within the geological history of Earth, the European Alps are a relatively young orogeny. They record the convergence of the African and European plates which created subduction zones and swallowed up ancient oceans and microcontinents until the major continental blocks collided with each other – tectonic processes which started in the Cretaceous and are still ongoing today (Schmid et al., 2022). Therefore, the Western Alps represent a collisional orogenic wedge where both ocean- and continent-derived tectonic units are exposed.

2.1 Evolution of the Alps

During the breakup of the supercontinent Pangaea, plate tectonic processes caused small ocean basins as well as microcontinents to form. One of these microcontinents was the so-called Briançonnais microcontinent, a submarine rise composed of the Corsica–Sardinia–Briançon continental fragments that can still be traced today from the Western Alps through to the Swiss Alps. It was framed to the northwest by the Valais Basin and to the southeast by the Piemonte-Liguria Ocean and the Penninic Ocean (Fig. 1). Located at the distal edge of the European continental margin, it was completely flooded in the Turonian (90 Ma) which led to the deposition of pelagic marly limestones (Pfiffner 2014). This microcontinent is sometimes also called Briançon Rise, microcontinent of the Briançon Rise or Briançonnais terrane (e.g., Pfiffner 2014). However, the widely accepted term "Briançonnais microcontinent" will be used throughout this thesis.

Most models propose that the subduction of the European plate under the Adriatic plate and the subsequent accretion and collision processes happened in two stages.

First, the Piemonte-Liguria Ocean was slowly subducted beneath the Adriatic plate during the Cretaceous in an east-to-SE dipping direction (Bachmann et al., 2009). This caused the Adriatic continental margin to be compressed into nappes and uplifted, while the European continental margin remained more or less passive (Pfiffner 2014).

Later, in the Cenozoic, the movement of the continental plates changed into a predominantly north-south direction. This caused the Briançonnais microcontinent to collide first with the Adriatic continental margin and then with the European continental margin, closing the Valais Basin in the process. Only the crystalline basement (upper crust) of the Briançonnais microcontinent was subducted; its cover sediments were sheared off and remained stuck near the surface. At this point, the European margin started to become dismembered and compressed into nappes as well and, over time, ever more external parts of the European margin were affected by this process of deformation. When the actual European continent ultimately collided with the African continental plate in the form of a non-subductable slab of continental crust with a thickness of about 30 kilometres, further nappe stacking took place in which upper crustal pieces were pushed upward along dipping thrust faults on both the European and the African plate margins (Pfiffner 2014).

Both the change of direction of the plate movements and the irregular form of the plate boundaries and continental margins contributed to the rather complex geometry which the Alps display today.

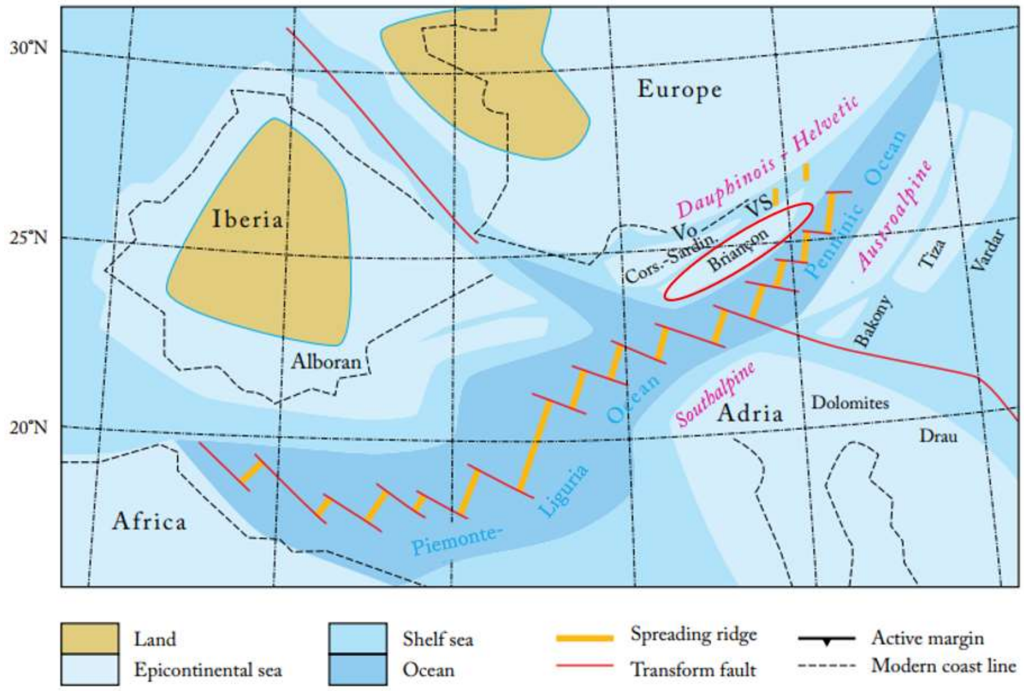

Fig. 1 Simplified plate reconstruction for the Early Cretaceous (ca. 125 Ma ago). The location of the Briançon microcontinent is highlighted (modified after Pfiffner 2014).

2.2 The Dora Maira Massif in the Western Alps

Today, the Alps are divided into four palaeogeographical-tectonic units: the southern Alps, the Austroalpine domain, the Penninic domain and the Helvetic domain. In general, the Penninic domain lies on top of the Helvetic towards the NW and the Austroalpine domain lies on top of the Penninic towards the SE (Fig. 2).

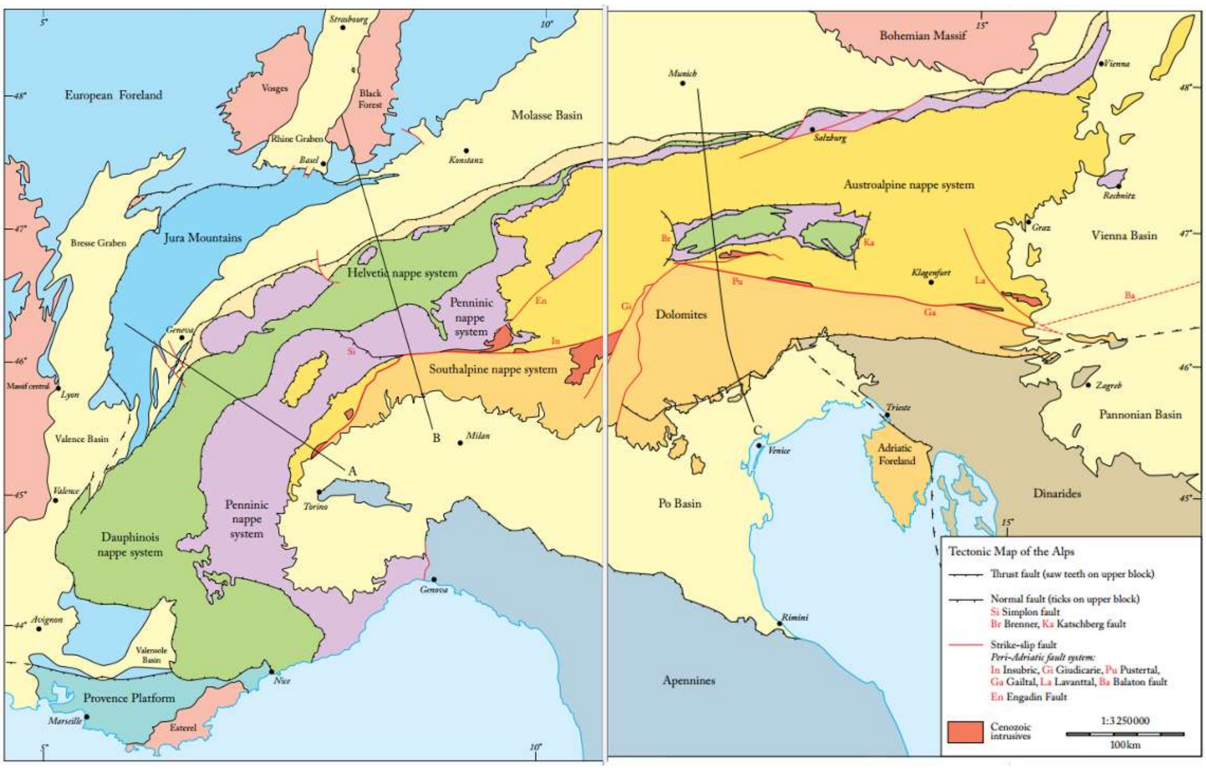

Fig. 2 Simplified tectonic map of the Alps and the distribution of nappe systems (modified after Pfiffner 2014).

Within a domain, belts of sedimentary rocks represent individual nappe complexes. A nappe complex consists of large crustal blocks that are thrust over each other and compressed during mountain building. As a general rule, higher units within a nappe stack are derived from palaeogeographically more internal parts of the original rocks (Pfiffner 2014).

The Western Alps run in a north-south direction, forming a tight arc around the western end of the Po Basin. Within this area, the Penninic domain is made up by nappes which consist of pre-Mesozoic granitoid and metamorphosed basement as well as a Permian-Mesozoic metasedimentary cover. It is widely exposed in southeastern France and northern Italy because erosion mostly removed the overlying Austro-Alpine nappes there (Miyashiro 1994). Furthermore, metamorphic rocks which formed at high pressure low temperature (HP-LT) are exceptionally well preserved in this area and indicate increasing *P-T* conditions from the westernmost to the easternmost units (Tajčmanová et al., 2021).

The Middle Penninic unit represents the former Briançonnais microcontinent within the Penninic nappe stack. It separates the North Penninic (representing the Valais Basin) from the

South Penninic (representing the Piemonte-Liguria Ocean) and consists of cover nappes, Palaeozoic sediments and crystalline nappes (Bachmann et al., 2009).

The Dora Maira Massif is one of the large crystalline uplifts within the Middle Penninic nappes of the Western Alps (together with the Gran Paradiso and Monte Rosa). It is located in the Piemonte region in the westernmost part of northern Italy and stretches for ~70 km from the Susa Valley in the north to the Maira Valley in the south (Fig. 3a). It is part of the so-called Internal Crystalline Massifs. Since it was formed by subduction of the Briançonnais microcontinent and the reworking of pre-existing crust, the Dora-Maira Massif, now stacked below the remnants of the Piemonte-Liguria Ocean, mainly consists of different tectonic units of Palaeozoic basement as well as minor remnants of dismembered Mesozoic covers. Metamorphic grade ranges from blueschist to eclogite facies (Manzotti et al., 2022).

The internal structure and geometry of the southern Dora Maira Massif is comparatively well researched, and several tectonic units have already been identified on the basis of petrological, lithological and structural observations (Fig. 3b). They are separated by thrust sheets as well as slivers of ophiolites and Mesozoic meta-sediments and the metamorphism reached ranges from garnet-blueschist to quartz-eclogite to coesite-eclogite facies. Moreover, Alpine peak *P-T* conditions for the lowermost unit have been estimated at 14–16 kbar and 400–500 °C or 20–23 kbar and 500–515 °C (Manzotti et al., 2022).

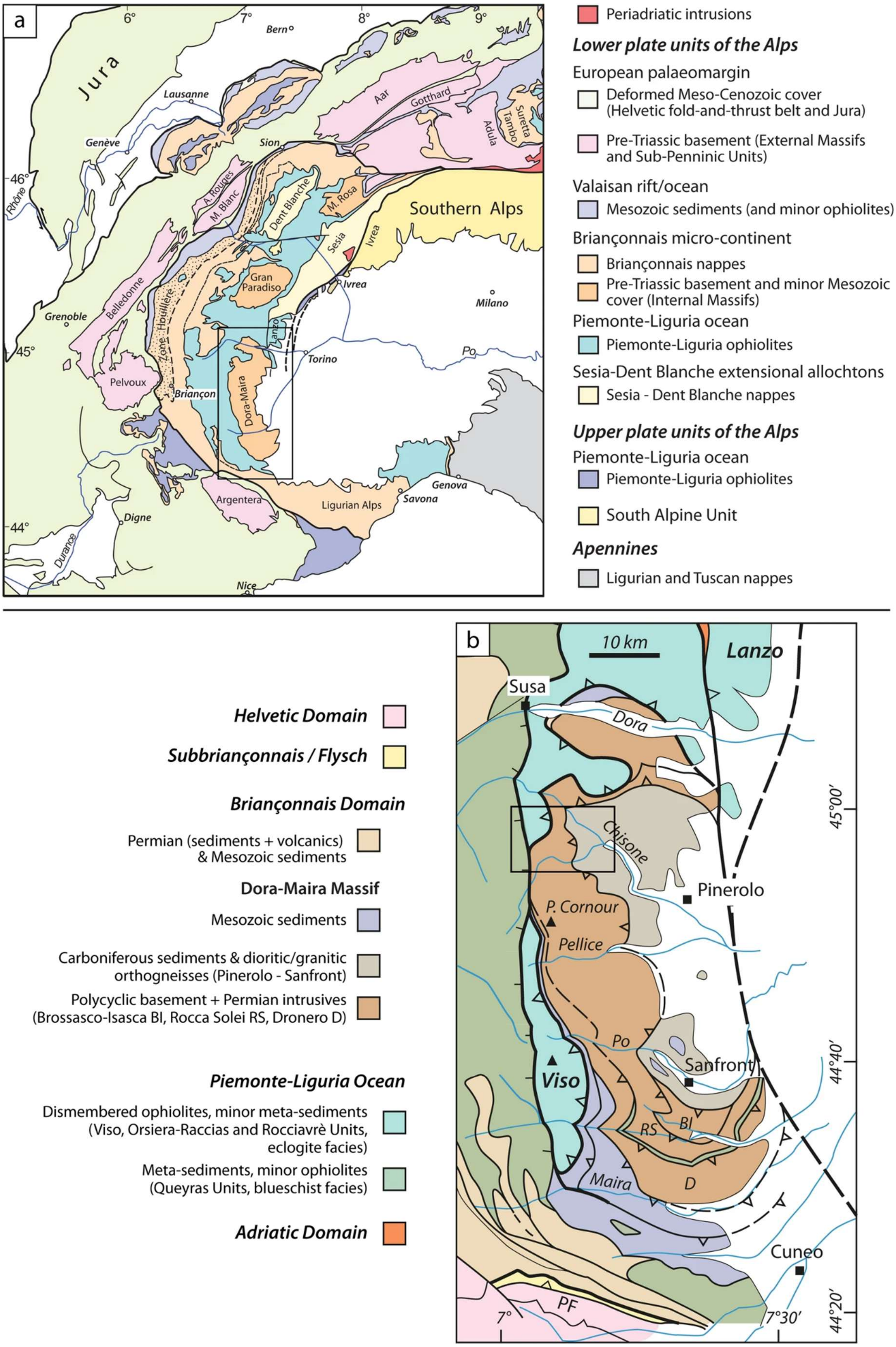

Fig. 3 a Simplified geological and structural map of the Western Alps. The black rectangle indicates the location of the tectonic map of **b**. **b** Tectonic map of the Dora Maira Massif (modified after Nosenzo et al., 2024). The black rectangle indicates the location of the geological map of **Fig. 4.**

2.3 The northern Dora-Maira Massif

Comparatively little is known about the metamorphic history and structural architecture of the northern Dora-Maira Massif. From bottom to top, the nappe stack currently consists of the following units (Figs. 4, 5):

The **Pinerolo Unit** is the structurally deepest unit of the nappe stack and records Upper Carboniferous graphite-rich metasediments which were intruded by Permian granites and diorites (Manzotti et al., 2016). Although Alpine metamorphic conditions have already been estimated for its southern part, no Alpine peak *P-T* estimates have been done for its northern sector yet. However, it is generally considered to belong to the upper blueschist facies (Manzotti et al., 2022).

The **Chasteiran Unit** has recently been identified as an ultrahigh-pressure metamorphism (UHP) unit lying between the Pinerolo and the Muret Unit. It is a thin layer (10-50 m thick) of graphite-rich garnet chloritoid micaschists possibly derived from black shales of Silurian age. It is discontinuously exposed in the immediate hangingwall of the Pinerolo Unit. Thermodynamic modelling on the basis of inclusions in garnet (chloritoid, rutile, coesite) indicates peak *P-T* conditions at 27-28 kbar, 510-530 °C. These metamorphic conditions are rare among the other UHP terranes around the world. They suggest that the Chasteiran Unit is the coldest Alpine unit known so far in the Alps and could represent a slice that was detached from the downgoing slab during subduction (Manzotti et al., 2022).

On top of the Chasteiran Unit lies the **Muret Unit** which represents a layer of Palaeozoic basement that tectonically overthrust both units below (Pinerolo and Chasteiran). It consists mainly of polycyclic rocks such as garnet-chloritoid micaschists, marbles and minor meta-basites together with an Ordovician biotite orthogneiss (so-called Muret orthogneiss). Metamorphic peak *P-T* conditions have been estimated at 21-22 kbar and 530-560 °C (Nosenzo et al., 2023).

On top of the Muret Unit, a new unit, the **Serre Unit**, has recently been identified (Manzotti et al., 2022; Nosenzo et al., 2024).

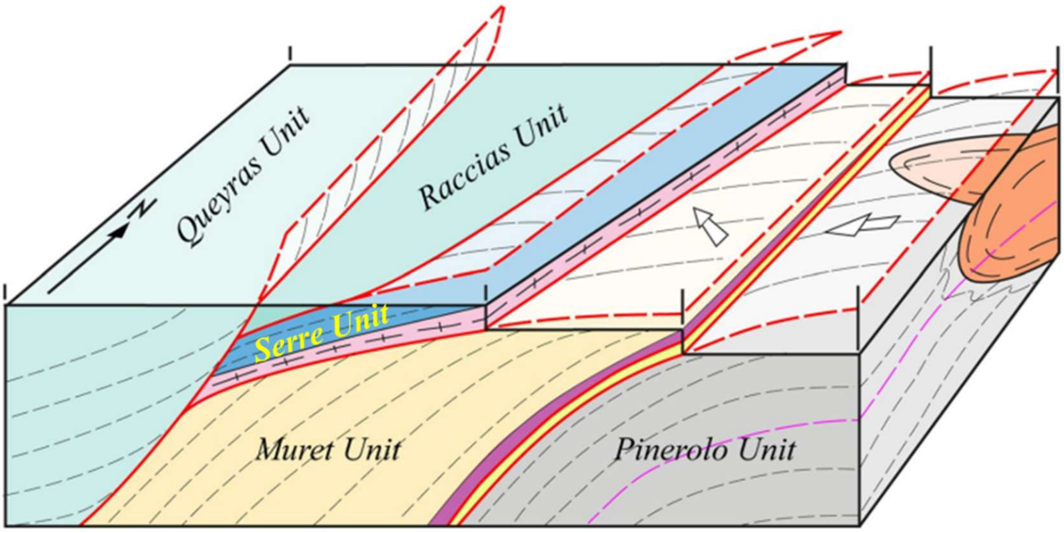

Fig. 4 Schematic sketch of the tectonic architecture of the northern Dora-Maira Massif. The Serre Unit is marked in bright yellow and consists of the two slices marked in blue and pink. The yellow thin slice between the Pinerolo and the Muret Units is the Chasteiran Unit (modified after Nosenzo et al., 2024).

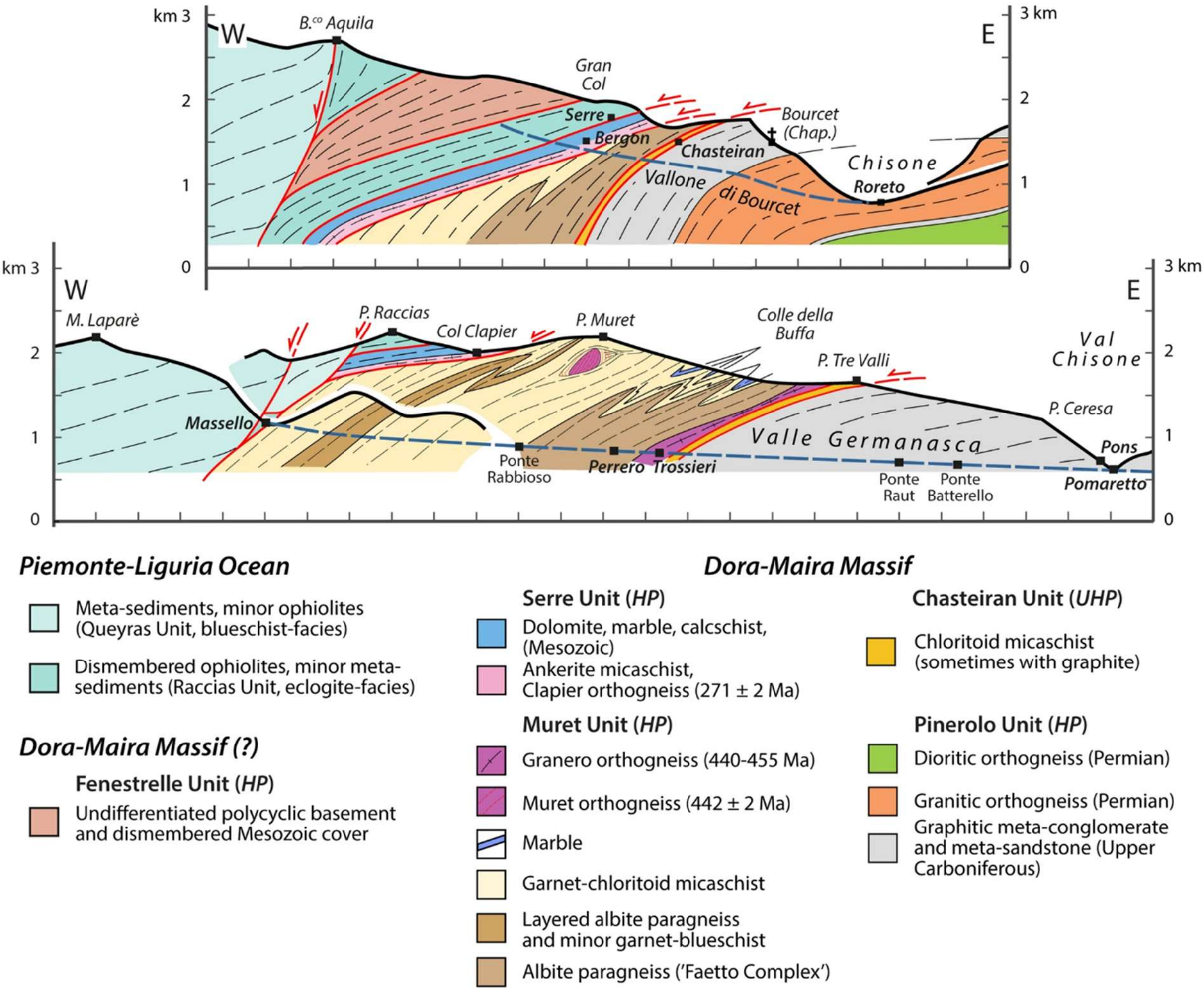

Fig. 5 Two schematic cross-sections of the northern Dora-Maira Massif. Tectonic boundaries are shown in red. The trend of the main, regional, foliation is indicated by thin, dashed, lines (modified after Manzotti et al., 2022).

2.4 The Serre Unit

The Serre Unit crops out discontinuously in the northern Dora-Maira Massif, bordering the oceanic units that were derived from the former Piemonte-Liguria Ocean. Geographically, the unit reaches ~350 m into the Bourcet Valley and thins out to a thickness of only a few tens of meters at Serrevecchio. It is overlain by the eclogite-facies ophiolites of the Raccias Unit. At Rocca Galmount, it is in direct contact with the blueschist-facies meta-sediments of the Queyras Unit (Nosenzo et al., 2024; Fig. 4).

Preliminary observations indicate that the Serre Unit includes several different lithologies which form tectonically juxtaposed lenses and discontinuous layers of variable size. In detail, the Serre Unit consists of Permian-age plutonic, volcanic and volcano-clastic rocks together with remnants of a dismembered Mesozoic cover which contains mainly orthogneisses, dolomites, marbles and minor calcschists as well as different types of micaschists (Manzotti et al., 2022). The dolostones, calcschists and marbles are covering the Permian magmatic and sedimentary rocks, and this carbonate-bearing sequence is characteristic of the Mesozoic cover in general. No fossils have been found in the carbonate-bearing rocks yet, but some were found in similar lithologies both north and south of the Serre Unit. The micaschists occurring in the Serre Unit include ankerite-bearing micaschists, silvery micaschists, quartz-rich micaschists with large (up to 8 mm long) pseudomorphed sodic amphibole and minor garnet-chloritoid micaschists (Fig. 6).

An analysis of rock samples collected from two different outcrops of the Clapier Orthogneiss in the Serre Unit indicates either a granite or a rhyolite protolith. Zircon crystals were found in one of the two samples and some of them contained an inherited core. Dating of four of these inherited cores using U/Th ratio analysis yield apparent ages at 348 ± 13 Ma, 378 ± 14 Ma, 679 ± 24 Ma and 1945 ± 34 Ma. Other ages found yield mainly discordant values between 210– 274 Ma. However, six (out of 22) dated samples yield concordant values and define a concordia date at 270.5 ± 1.8 Ma (Nosenzo et al., 2024).

In the Germanasca valley, the Serre unit is characterized by a pervasive ductile deformation and its tectonic structure indicates that it is separated at its footwall by a narrow shear zone, the ductile to brittle La Fracho Shear Zone (Nosenzo et al., 2024).

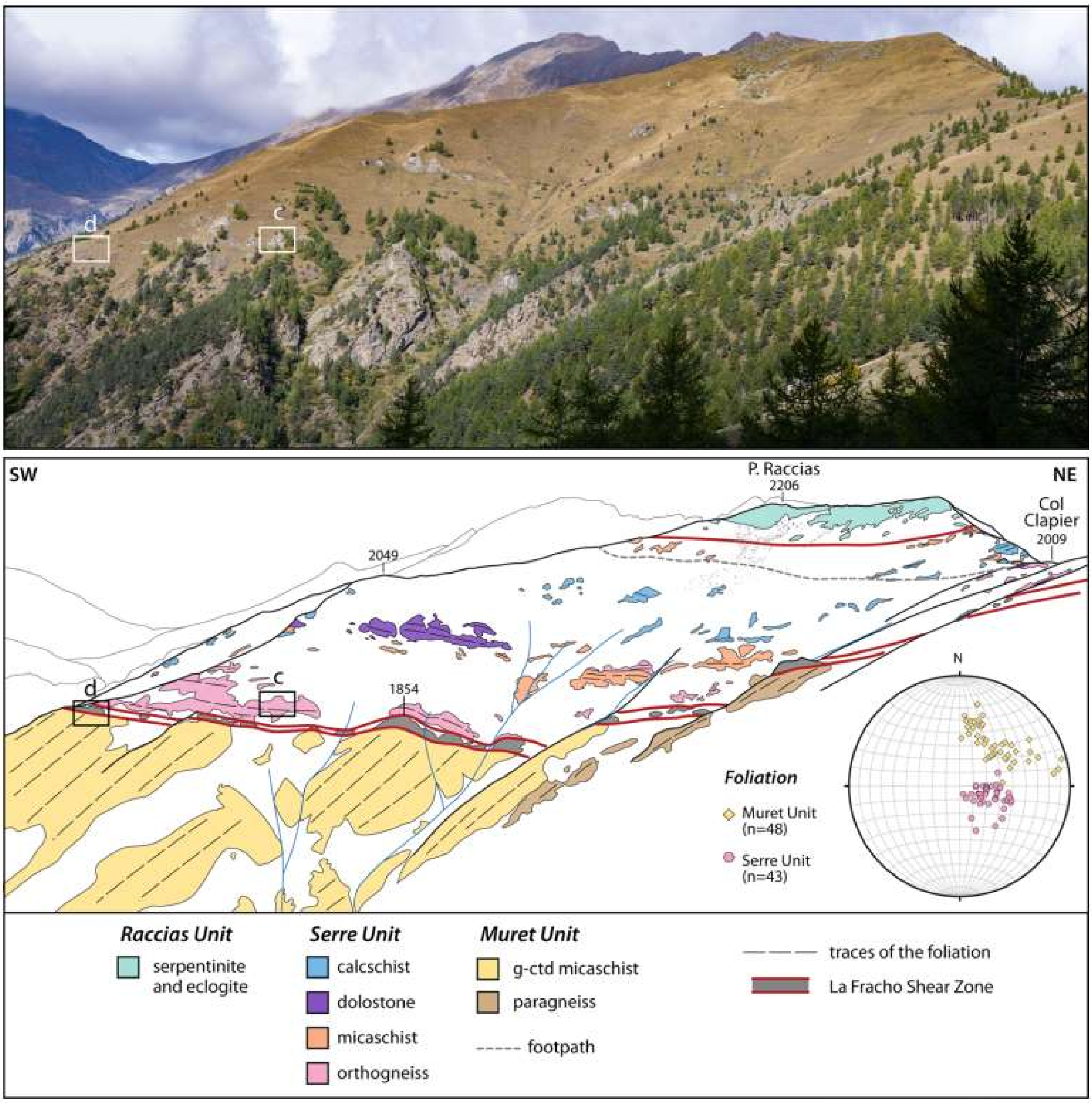

Fig. 6 Panorama of the SE slope of the Col Clapier and Punta Raccias. The main foliation in the Muret and Serre Units displays a different average orientation (see the lower hemisphere Schmidt (equal-area) projection of the main foliation). The tectonic boundary between the Muret and Serre Units is marked by zone of intense deformation (i.e. La Fracho Shear Zone) characterised by CS structures (modified after Nosenzo et al., 2024).

This study focuses on the Mesozoic cover of the Serre Unit. Its main goal is to contribute a hypothesis about its tectonometamorphic evolution based on the petrographic analysis of 10 thin sections. The studied samples were collected close to each other at the location highlighted in Fig. 7.

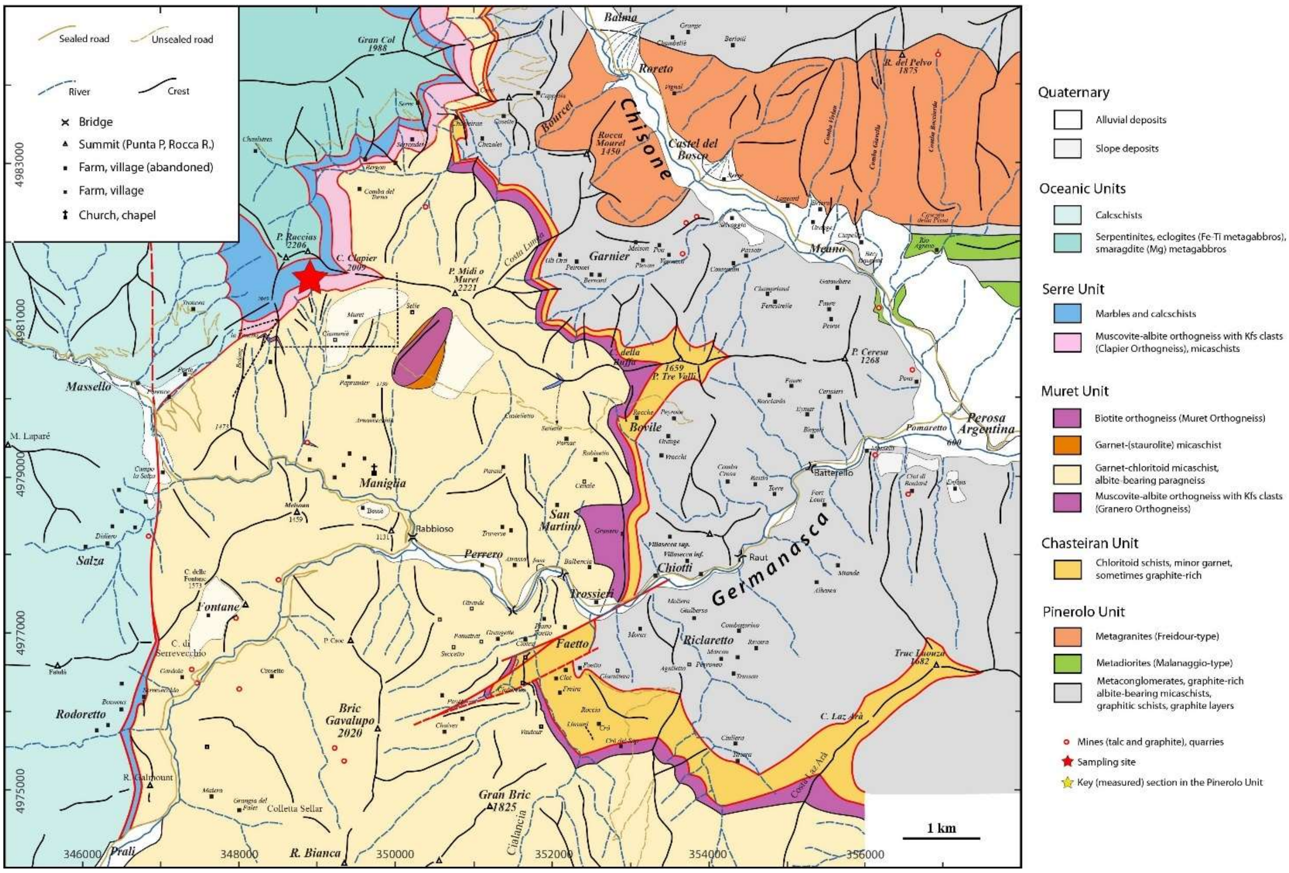

Fig. 7 Simplified tectonic map of the northern Dora Maira Massif. The red star marks the location of the studied samples (modified after Nosenzo et al., 2024).

3. Methods

This study focuses on the petrographic analysis of 10 thin sections from the Serre Unit. All optical observations were conducted at Stockholm University.

The thin sections were scanned both in cross-polarised light (XPL) and plane-polarised light (PPL) using a Nikon Coolscan 9000. Full-resolution images of the scans are provided digitally.

The abundance of minerals was estimated both by image analysis of the scanned thin sections and by using the MSAG Universalsichtgerät nach Klaus.

The petrographic analysis was performed using a Leica DMLSP microscope and microphotographs were taken with a Leica MC170 HD camera. The minerals present in the different samples were identified and described in detail, together with evidence of relict minerals and mineral reactions. Additionally, microstructures (e.g. foliations, microfolding, fractures, pressure shadows, remnants of pseudomorphs) were used to reconstruct a sequence of mineral growth/dissolution in each sample. These detailed descriptions allowed identification of different Alpine tectonometamorphic stages of the Serre Unit.

A high concentration of zoned chloritoid was found in two thin sections and investigated in greater detail. The zoned area was measured in 15 randomly selected crystals for each thin section using the software ImageJ.

The peak mineral assemblage observed in the studied samples was compared to pressure-temperature (*P-T*) pseudosections and corresponding mineral assemblages of two similar tectonic units situated in the direct vicinity of the Serre Unit. An estimation of *P-T* conditions was done by localizing the field in the respective pseudosection that had the same mineral assemblage as the samples studies here. Further constraints were placed by comparing mineral isopleths with the mineral assemblage. The results were assessed critically and a plausible range for peak *P-T* conditions for the Serre Unit was determined.

Finally, both the identification of different tectonometamorphic stages and the estimated range of peak *P-T* conditions were used to propose a hypothesis about the tectonic evolution of the Serre Unit.

Abbreviations used in this text are listed below (Table 1). Mineral abbreviations after Holland and Powell (2011).

Mineral	**Abbreviation**	**Other terms**	**Abbreviation**
Muscovite	mu	Pressure and Temperature	*P-T*
Paragonite	pa	Specific foliations	S_i
Quartz	q	Weight percent	wt%
Jadeite	jd		
Glaucophane	gl		
Garnet	g		
Chloritoid	ctd		
Albite	ab		
Calcite	cc		
Rutile	ru		
Ilmenite	ilm		
Chlorite	chl		
Lawsonite	law		
Epidote	ep		
Graphite	gph		

Table 1: Abbreviations of minerals and other terms used in the text.

4. Results

4.1 Petrography of the studied samples

Ten samples from the Serre Unit were studied by optical microscopy:

- Garnet-chloritoid micaschist (samples highlighted in yellow in Table 2)
- Chloritoid micaschist with little or no garnet (samples highlighted in blue in Table 2)
- Calcschist (two samples highlighted in violet in Table 2)
- Marble (one sample highlighted in orange in Table 2)

Since it is not possible to distinguish between muscovite and paragonite by optical microscopy alone, no distinction will be made between muscovite and paragonite in the following descriptions. These minerals will all be treated as white mica.

The estimated mineral composition of the different samples is given in Table 2.

Mineral	GM2147	GM2160A	GM2160B	**Avg.**	GM1905	GM1906	GM1907	GM2161	**Avg.**
Quartz (q)	30%	20%	35%	28%	25%	15%	25%	25%	23%
Muscovite (mu)	45%	60%	25%	43%	15%	25%	30%	25%	24%
Chlorite (chl)	5%	<5%	5%	<5%	<5%	10%	5%	5%	7%
Chloritoid (ctd)	15%	10%	15%	13%	45%	35%	25%	30%	34%
Garnet (g)	<5%	5%	10%	8%	<5%	-	-	<5%	<5%
Albite (ab)	<5%	<5%	<5%	<5%	-	<5%	-	5%	<5%
Glaucophane pseudom. (gl)	-	<5%	5%	<5%	10%	5%	10%	5%	8%
Calcite (cc)	-	-	-		-	-	-	-	
Rutile (ru)	<1%	<1%	<5%	<5%	<5%	5%	<5%	<5%	<5%
Ilmenite (ilm)	<1%	<1%	<1%	<1%	<1%	<1%	<1%	<1%	<1%
Epidote (ep)	-	-	-		<1%	-	-	-	<1%
Graphite (gph)	<1%	<1%	-	<1%	<1%	<1%	<1%	<1%	<1%

Mineral	CH2016	GM1903	**Avg.**	GM2025
Quartz (q)	10%	15%	13%	-
Muscovite (mu)	10%	5%	8%	<1%
Chlorite (chl)	5%	-	5%	<5%
Chloritoid (ctd)	-	-		-
Garnet (g)	-	-		-
Albite (ab)	5%	-	5%	-
Glaucophane pseudom. (gl)	-	-		-
Calcite (cc)	65%	80%	73%	95%
Rutile (ru)	<5%	<1%	<5%	-
Ilmenite (ilm)	-	-		-
Epidote (ep)	-	-		-
Graphite (gph)	<5%	<1%	<5%	<1%

Table 2: Mineral percentages estimated in the different samples.

Differences in mineral modal amount in the studied samples

The studied metapelites mainly differ in the modal amount of chloritoid and garnet (Table 1 and Fig. 1). The amount of chloritoid is low (10-15 %) in samples GM2147, GM2160A and GM2160B, while garnet is quite abundant (up to 10%). Therefore, these three samples can be named garnet-chloritoid micaschist.

Samples GM1905, GM1906, GM1907 and GM2161 are very rich in chloritoid and contain minor (<5%) or no garnet. These samples can therefore be called chloritoid micaschist (Fig 8).

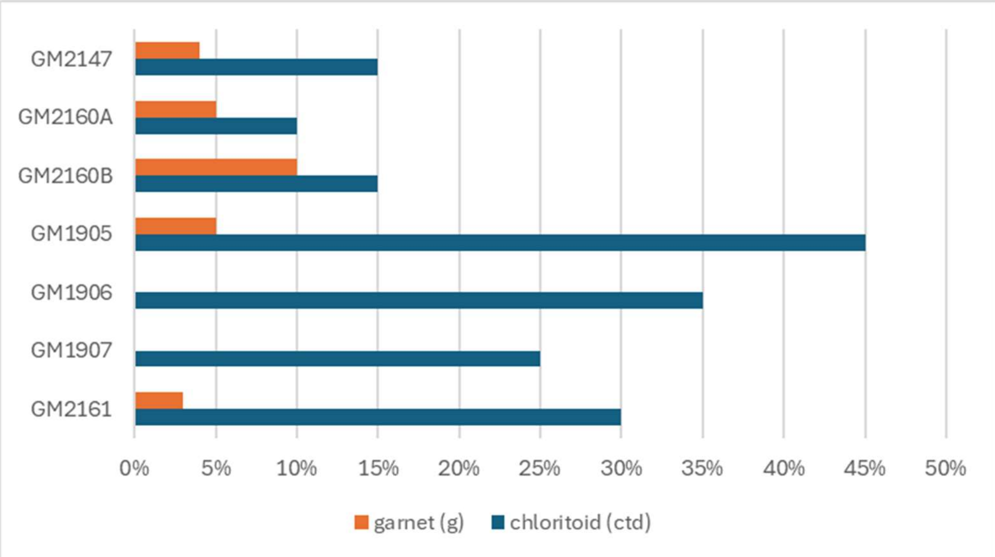

Fig. 8 Comparison of modal amounts of garnet and chloritoid in the studied metapelites.

Garnet-chloritoid micaschist

The first tectonometamorphic stage (**stage 1,** Fig. 9) recognised in these rocks comprises unoriented minerals included in garnet and chloritoid. Inclusions in garnet consist of quartz, rutile, chloritoid, and white mica. The most common inclusions are quartz and rutile. Chloritoid inclusions are mainly found in the garnet core while quartz, white mica and rutile occur both in the core and in the rim. Exceptionally large chloritoid inclusions containing sparse graphite and other optically unidentifiable minerals are observed in garnet porphyroblasts in sample GM2160A (Fig. 10). Finally, matrix chloritoid also contains a few inclusions of graphite, rutile, and white mica.

Stage 2 is associated with the development of the main foliation (S_1) defined by mm-thick layers of either chloritoid + graphite + rutile or white mica + rutile + graphite ± chlorite, which are parallel to stretched quartz-rich lenses. The main foliation is also defined by the shape preferred orientation of white mica and chloritoid and is wrapping around the garnet porphyroblasts.

Garnet porphyroblasts range in size from 0.7 to 5 mm. The largest crystals are observed in sample GM2160B (size up to 5 mm). Pressure shadows are observed around one or both sides of some of the garnet porphyroblasts and contain white mica, quartz and rutile (Fig. 11).

Overall, the S_1 foliation is more pervasive in sample GM2147 than in samples GM2160A and GM2160B. In sample GM2160A, the S_1 foliation is microfolded (Fig. 12).

Apart from defining the main direction of foliation, some white mica crystals are also attenuated in the direction of shearing, forming a shape known as “mica fish” (Van der Pluijm 2004; Fig. 13).

Rhomboidal domains (interpreted as pseudomorphs after glaucophane, e.g. Manzotti et al., 2022) are oriented parallel to S_1 foliation. Glaucophane pseudomorphs display a range of shapes, varying from euhedral to anhedral. They occur in the quartz-rich lenses and sometimes in the white mica layers.

Rutile also occurs in the matrix and can often be found in clusters at the edge of chloritoid.

Stage 3 is characterised by the static replacement of minerals and brittle deformation. For instance, the replacement of glaucophane described above occurs during this stage. When glaucophane is dissolved, Fe and Mg are used in the formation of chlorite, while Na is used to form albite. Thus, glaucophane is replaced by fine-grained aggregates consisting of chlorite, albite and amphibole. Inclusions of oxidised chlorite and ilmenite are present in some of the pseudomorphs.

Garnet porphyroblasts are highly fractured, partially dissolved at the rim and replaced by chlorite (Fig. 5). Fractures are randomly oriented and discordant with respect to the S_1 foliation, indicating that they post-date the development of the main S_1 foliation. Fractures are locally filled by chlorite ± white mica. It worth to note that garnet chloritization is more pervasive in samples GM2160A and GM2160B than in sample GM2147.

Chloritoid inclusions in garnet surrounded by cracks are partly replaced by chlorite at the rim (Fig. 10).

Rutile is present in the matrix and also as inclusions in garnet. Some of the rutile inclusions in garnet are surrounded by cracks and display ilmenite coronas (Figs. 14, 15).

Rare albite dispersed in the matrix also grows during this stage.

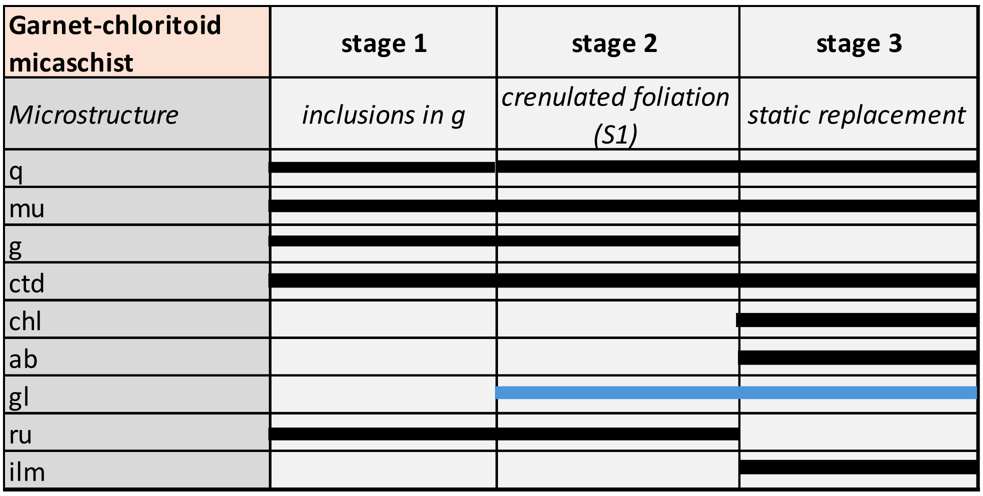

Fig. 9 Relationships between mineral growth and deformation for the garnet-chloritoid micaschist. The blue line indicates pseudomorphed minerals.

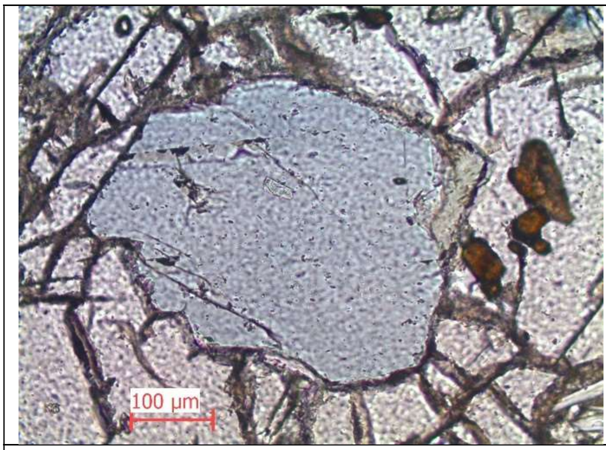

Fig. 10 Chloritoid inclusion in garnet surrounded by cracks and partly replaced by chlorite (PPL).

Fig. 11 Pressure shadow around garnet containing white mica, quartz and rutile (PPL).

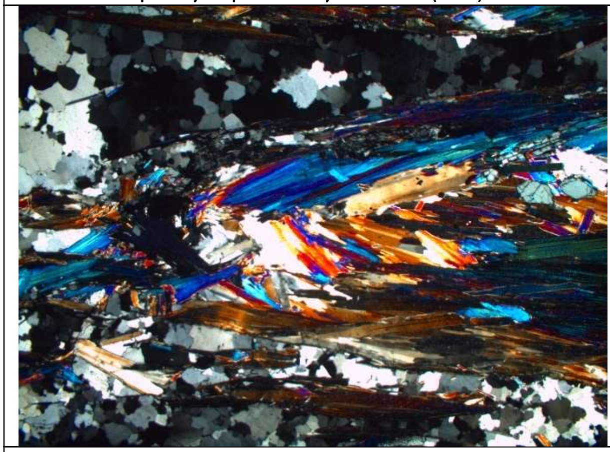

Fig. 12 Microfold in white mica surrounded by quartz (XPL).

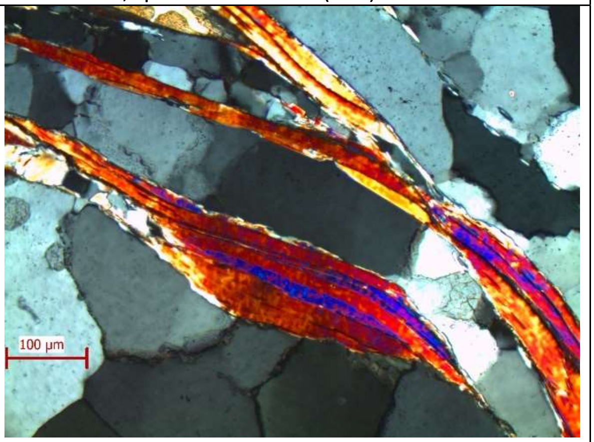

Fig. 13 Close-up of mica fish in matrix of quartz (XPL).

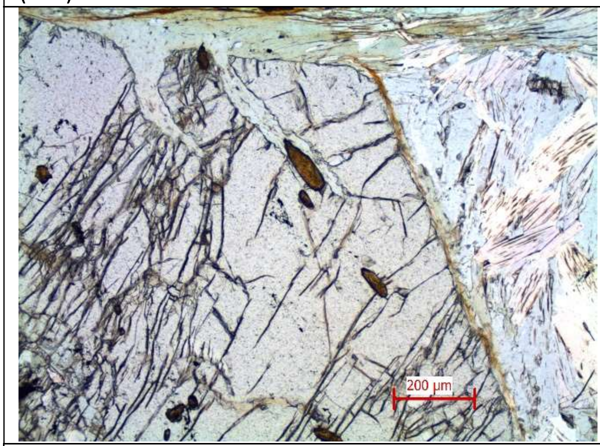

Fig. 14 Inclusions of rutile in garnet. Note that the fractures in garnet are filled with chlorite (PPL).

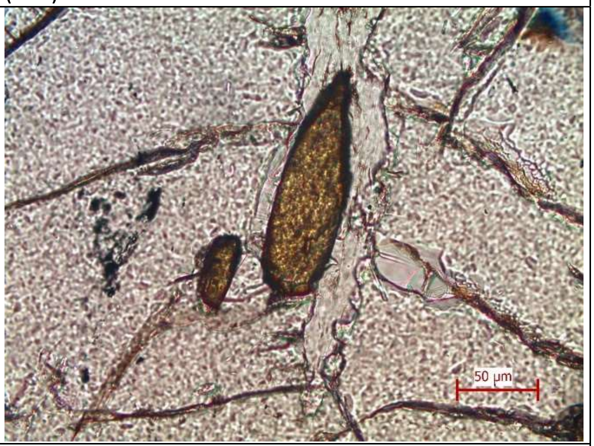

Fig. 15 Close-up of the largest inclusion of rutile (Fig. 14) with dark corona of ilmenite (PPL).

Chloritoid micaschist

The first tectonometamorphic stage (**stage 1,** Fig. 16) in this group is mainly defined by unoriented minerals included in chloritoid and garnet. Inclusions in chloritoid consist of quartz, white mica, rutile and graphite. The most common inclusions are rutile and graphite (Fig. 17). Quartz and white mica inclusions are mainly found in the chloritoid core while rutile and graphite occur both in the core and in the rim. One inclusion of zircon was found in sample GM1907 (Fig. 18). When present, garnet contains inclusions of quartz, white mica and rutile. Finally, white mica in the matrix locally contains inclusions of graphite.

As in the garnet-chloritoid micaschists, **stage 2** is associated with the development of the main foliation (S_1) defined by mm-thick layers of either chloritoid + graphite + rutile or white mica + rutile + graphite ± chlorite, which are parallel to stretched quartz-rich lenses. The main foliation is also defined by the shape preferred orientation of chloritoid and white mica. When garnet is present, S_1 is wrapping around the garnet porphyroblasts and pressure shadows are detectable on one or both sides, containing white mica, quartz and rutile.

The S_1 foliation is microfolded in almost all of the samples. Notably, microfolding is more pronounced in this group than in the garnet-chloritoid micaschists (Fig. 19).

Offset of both of the garnets suggests that shear stress was more pronounced in this group than in the garnet-chloritoid micaschists and caused deformation of the garnets (Fig. 20).

In this rock, chloritoid is one of the most abundant minerals. It makes up 25-45% of the mineral composition with individual crystals ranging from 0.1 to 1.2 mm in size. Apart from defining the main direction of foliation, most chloritoid crystals are zoned with a lighter-blue core and a darker-blue rim (Fig. 21), suggesting a Mg-richer core and a Mg-poorer rim. The zoned rims probably developed during this stage and will be discussed in more detail below.

As in the garnet-chloritoid micaschists, rhomboidal domains (interpreted as pseudomorphs after glaucophane) are oriented parallel to S_1 foliation. Glaucophane pseudomorphs are sub- to anhedral and occur in the white mica layers and sometimes in the quartz-rich lenses. Furthermore, rutile also occurs in the matrix and can often be found in clusters along the outer edges of chloritoid. It is worth to note that the amount of both glaucophane pseudomorphs and rutile in the matrix is higher in this group than in the garnet-chloritoid micaschists.

Stage 3 is characterised by replacement of minerals and brittle deformation. Chloritoid is fractured and in places partly dissolved at the rim and replaced by chlorite. When present, garnet porphyroblasts are also highly fractured and replaced by chlorite along their outer edges, similar to the garnets described in the garnet-micaschists above. In both chloritoid and garnet, fractures are randomly oriented and discordant with respect to the S_1 foliation, indicating that they post-date the development of the main S_1 foliation. Fractures in chloritoid are locally filled by chlorite ± white mica while fractures in garnet are filled by chlorite and quartz.

As in the garnet-chloritoid micaschists, glaucophane is replaced during this stage by fine-grained aggregates consisting of chlorite, albite and amphibole (Fig. 22).

Many of the rutile crystals display dark coronas of ilmenite, irrespective of their petrographic occurrence.

Small amounts of albite dispersed in the matrix also grow during this stage.

Rare epidote (Fig. 14) containing an inclusion of rutile is present in the matrix of one of the garnet-bearing chloritoid micaschists.

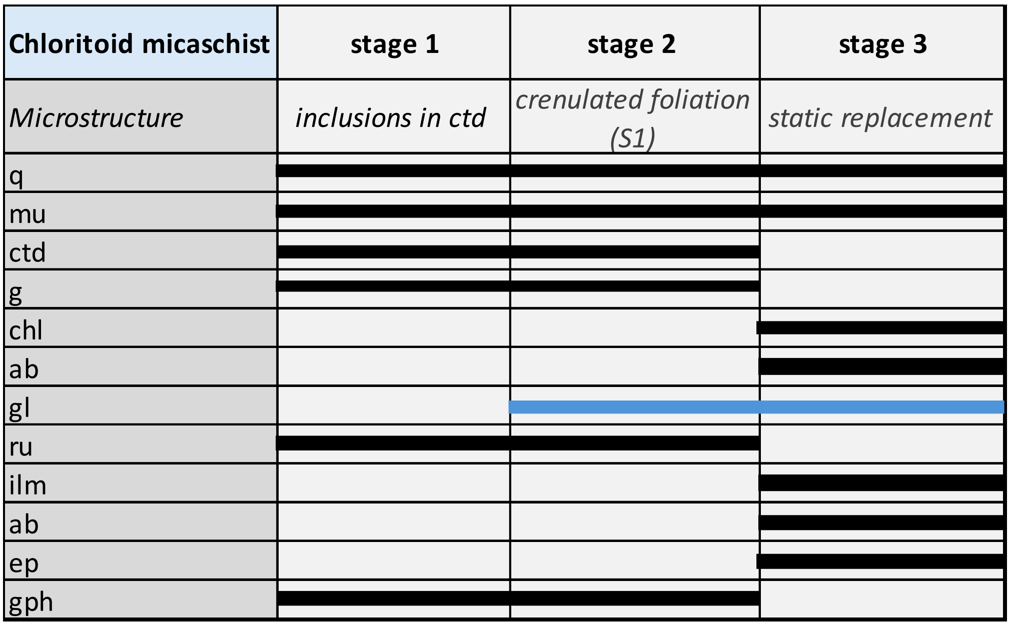

Fig. 16 Relationships between mineral growth and deformation for the chloritoid micaschist with little or no garnet. The blue line indicates pseudomorphed minerals.

Fig. 17 Chloritoid with inclusions of rutile and graphite in matrix of white mica and chlorite (PPL).

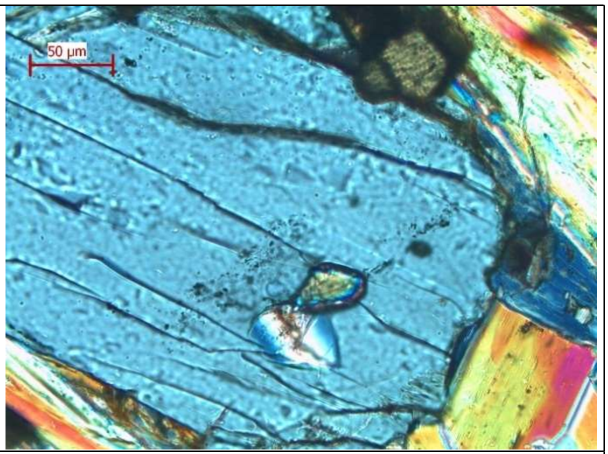

Fig. 18 Chloritoid displaying a large zircon inclusion and tiny dispersed graphite inclusions. The large crystal adjacent to the zircon is probably white mica (XPL).

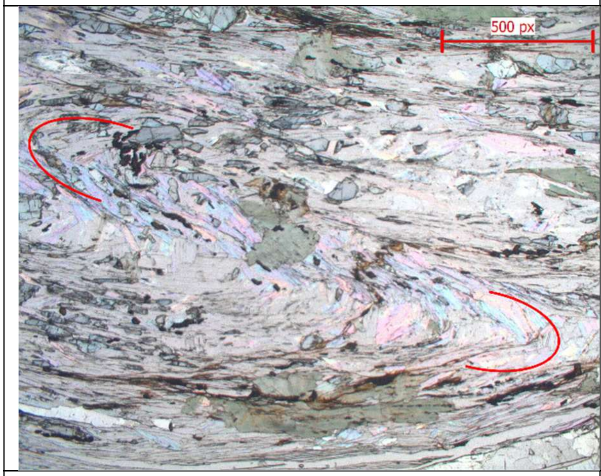

Fig. 19 Microfolding of white mica (PPL).

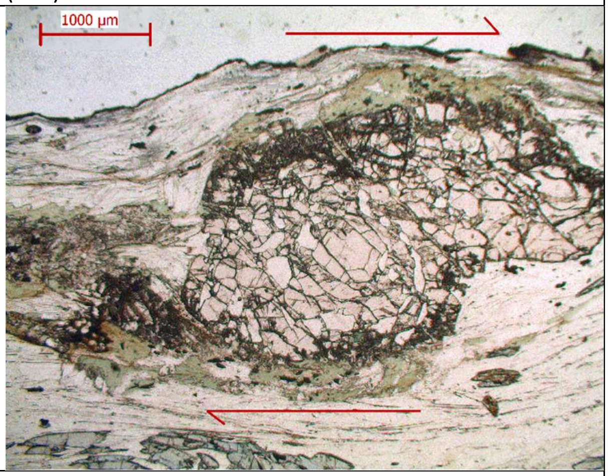

Fig. 20 Sense of shear in a highly fractured and partly chloritized garnet wrapped by foliated matrix containing quartz, white mica and rutile (PPL).

Fig. 21 Zoned chloritoid with inclusion of white mica. Epidote at the bottom left (PPL).

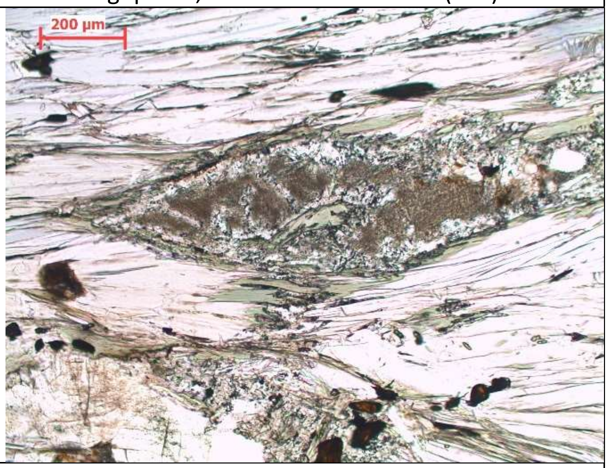

Fig. 22 Glaucophane pseudomorph with inclusions of rutile that are partly replaced by ilmenite (PPL).

To conclude, three Alpine tectonometamorphic stages can be identified for the Serre Unit. The stable mineral assemblage at peak metamorphism (stage 2) consists of quartz, white mica, garnet, chloritoid, glaucophane and rutile.

The main features of the carbonate rocks are briefly outlined below. Due to the poor mineralogy of these rocks, no tectonometamorphic stages were distinguished in these rocks.

Calcschist

Samples CH2016 and GM1903 are calcschist and mainly consist of calcite, white mica, albite, chlorite and discontinuous layers of quartz. Calcite crystals commonly contain randomly dispersed micro-inclusions of graphite (Fig. 23).

A weak matrix foliation is defined the shape preferred orientation of white mica. Interestingly, some of the white mica crystals are zoned in XPL, suggesting a change in chemical composition (e.g., Si, Mg, Fe, Al) (Fig. 24).

Albite crystals are dispersed in the matrix and frequently display graphite inclusions. The latter are also quite common in quartz, white mica and chlorite.

Finally, reddish-brown iron-oxides are observed in the matrix as well.

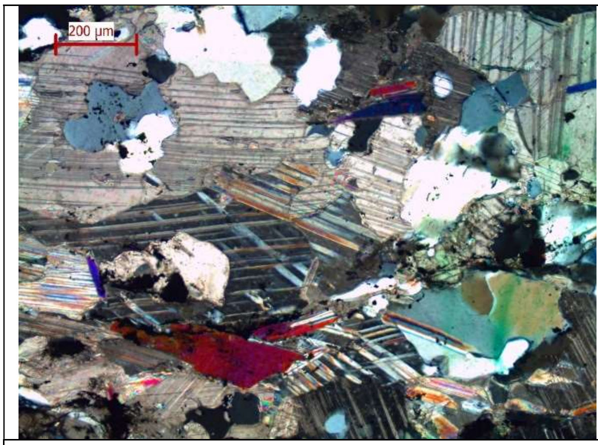

Fig. 23 Calcite with characteristic deformation twinning and inclusions of quartz, white mica, albite and graphite (XPL).

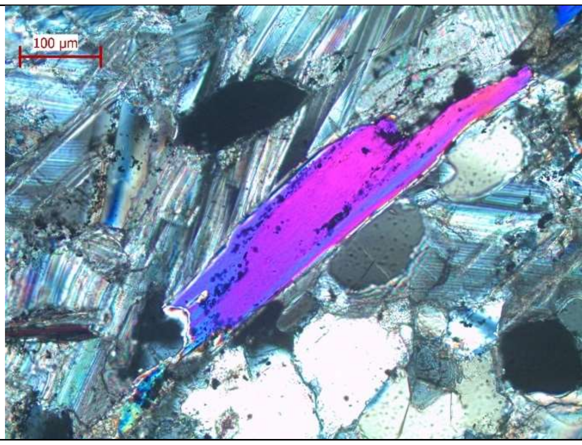

Fig. 24 Zoned white mica in a matrix of calcite and quartz (XPL).

Marble

Sample GM2025 is a polycrystalline rock consisting mainly of calcite with small amounts of chlorite, white mica and graphite. Traces of white mica are present in the matrix and fibrous chlorite is filling one fissure/vein.

Most of the crystals in this sample are oriented randomly. However, a very weak foliation is detectable in one area by slightly compressed grains which are oriented parallel to the direction of the vein (Figs. 25, 26).

Fig. 25 Scan of thin section GM2025. The vein is marked in red (PPL).

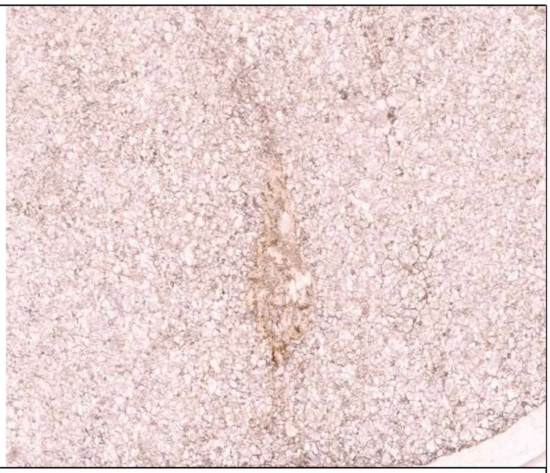

Fig. 26 Close-up of the vein and weak foliation oriented parallel to it (PPL).

4.2 Chloritoid zoning

As mentioned above, there are zoned chloritoid crystals present in some of the thin sections. The highest concentration of zoned chloritoid can be found in thin sections GM1906 and GM1907. These two thin sections were therefore carefully examined to better understand the zoning of this mineral.

The relative modal abundance of core and rim in chloritoid were determined on the basis of the following steps:

1. Measuring the total area occupied by 15 chloritoid crystal in samples GM1906 and GM1907
2. Measuring the area occupied by the rim in each chloritoid crystal.
3. Calculating the difference between the total area and the area of the rim in each chloritoid crystal.

The modal abundance of chloritoid previously estimated in the two samples (see Table 2) was used to calculate the relative proportion of chloritoid core and rims.

Sample GM1907 contains 25% of chloritoid, of which 20% corresponds to the area of the core domain and 5% to the area of the rim. Sample GM1906 contains 35% of chloritoid, 27% of which corresponds to the core domain, whereas 8% corresponds to the rim (Fig. 27).

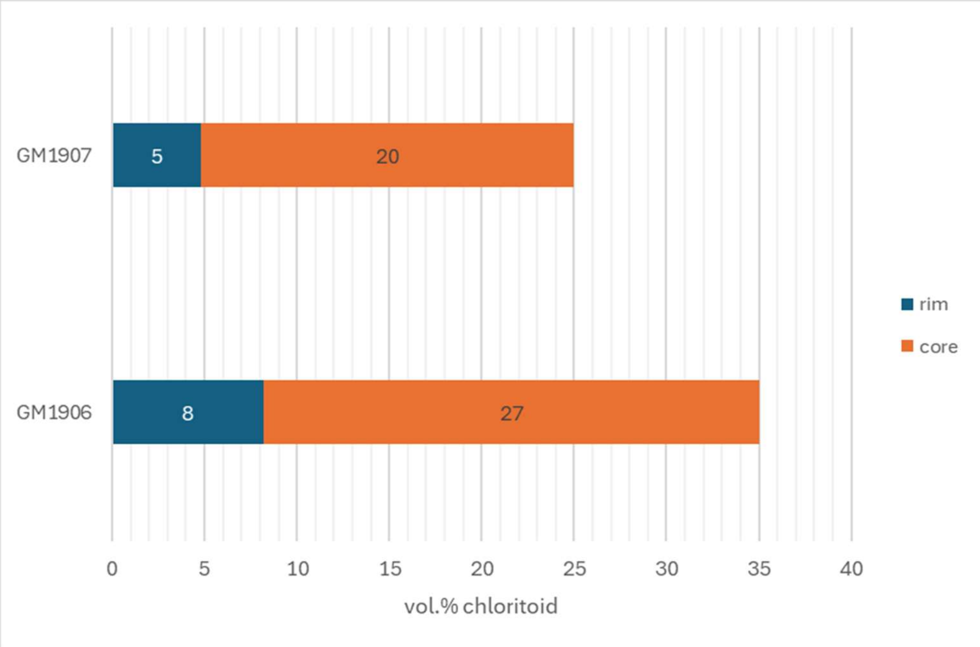

Fig. 27 Zoned rim vs. core in chloritoid.

Analysis of the zoned area in relation to the entire area of individual crystals suggests that, in both thin sections, the rims of the smallest chloritoid crystals (~0.2 mm) make up 35 – 50% of the entire crystal. It is important to note, however, that the selected small crystals represent sections cut through the external portion of the crystals (Fig 28).

By contrast, larger chloritoid crystals (up to 1.2 mm, Fig. 29) display relatively constant and small rim domains (21% for GM1906 and 19% for GM1907, respectively; Figs. 30, 31)

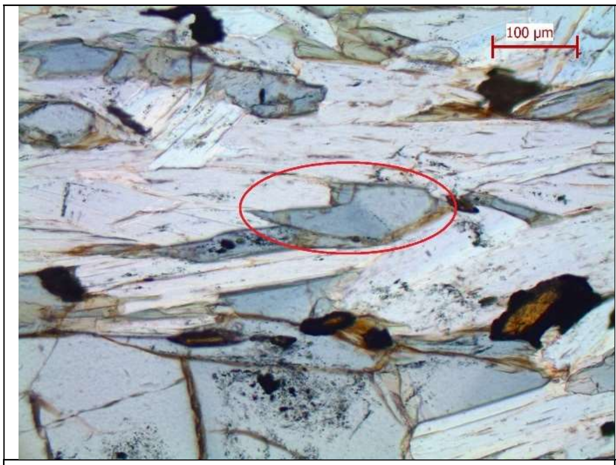

Fig. 28 Small chloritoid crystal representing part of a larger crystal (PPL).

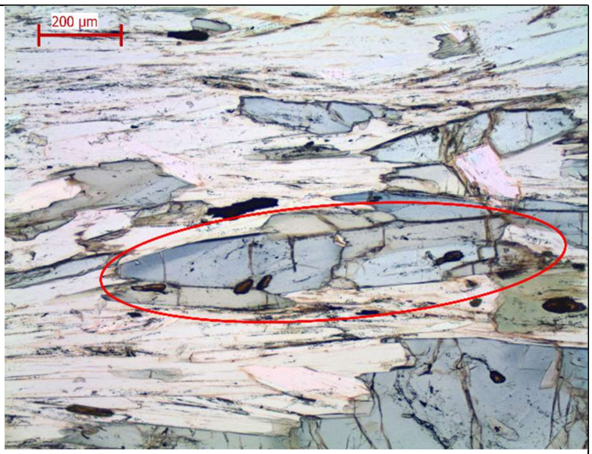

Fig. 29 Zoned area in one of the larger chloritoid crystals (PPL).

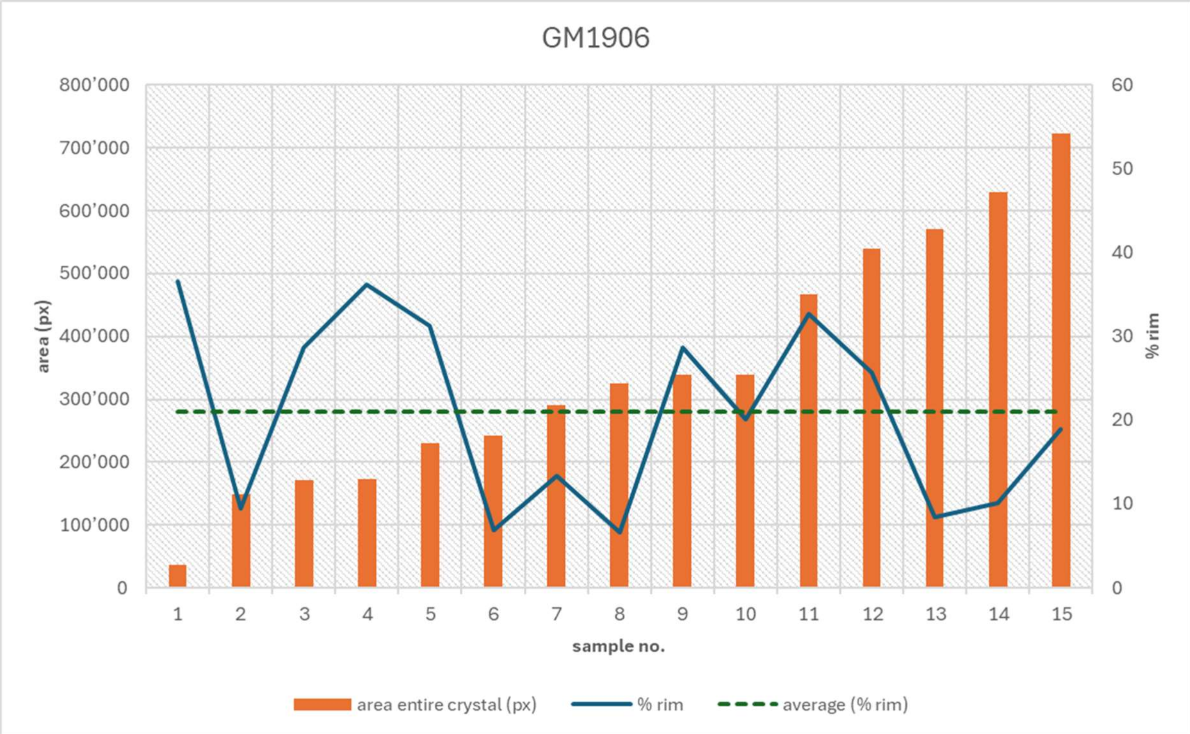

Fig. 30 Relationship between size of the examined crystals and zoning of the rim in GM1906.

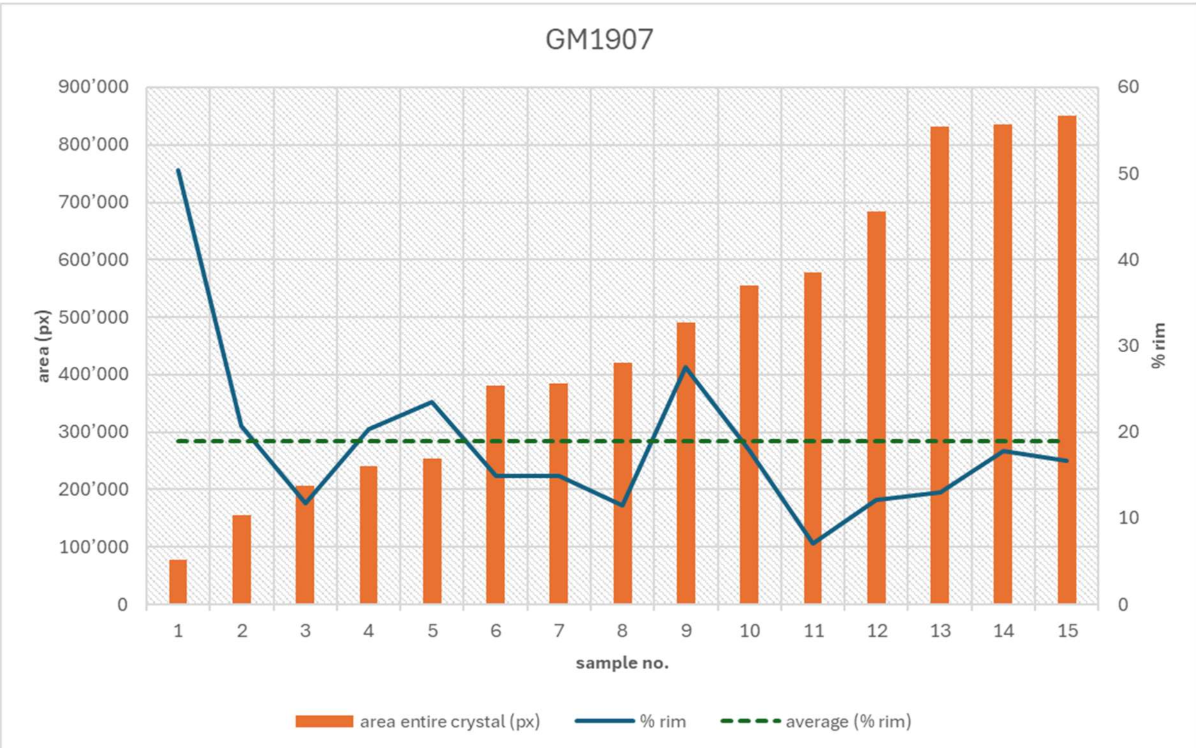

Fig. 31 Relationship between size of the examined crystals and zoning of the rim in GM1907.

5. Discussion

5.1 Metamorphic reactions

Based on the petrographic observations and comparison with previous studies on metapelites, a series of potential chemical reactions are briefly discussed below.

Garnet and chloritoid

Metapelites of the Serre Unit contain garnet and chloritoid. The growth of both garnet and chloritoid during prograde metamorphism of pelites can be modelled by the continuous dehydration reaction *chlorite + muscovite + quartz = garnet + chloritoid +* H_2O.

In the studied metapelites, garnet and chloritoid are partially replaced by chlorite. During retrograde metamorphism, exposition to fluids reverses the reaction described above, resulting in partial or complete replacement of garnet and chloritoid by chlorite (Nosenzo et al., 2023). The observed fractures in garnet are a path for fluid infiltration, favouring the partial replacement of chloritoid inclusions by chlorite and the precipitation of chlorite filling the fractures. Locally, white mica was also observed filling the fractures. This is peculiar, since K is needed to produce white mica, but garnet does not contain this element. However, the fluid penetrating in the garnet along the fractures could have facilitated the transport of K favouring the white mica formation.

Other reactions that produce either garnet or chloritoid could have occurred as well. Garnet growth in metapelites is often modelled by the dehydration reaction *chlorite + quartz = garnet +* H_2O. Since garnet and chlorite both belong to a solid solution series, this reaction can occur over a range of different temperatures (Philpotts and Ague 2022).

Chloritoid can be produced by the dehydration reaction *pyrophyllite + chlorite = chloritoid + quartz +* H_2O (Franceschelli et al., 1999). Chloritoid is stable in both low- and medium-grade metapelites. Moreover, its stability seems to expand with pressure as it is widely found in metamorphic rocks from high-pressure terranes that are high in Mg-content (Frost 2019).

Rutile and ilmenite

Minor amounts of rutile and ilmenite are present in the micaschists as the Ti-bearing phases. Rutile is almost always surrounded by a dark corona of ilmenite. Rutile and ilmenite can replace each other according to reaction: *rutile + iron +* O_2 *= ilmenite*. This reaction generally occurs during retrograde metamorphism.

Albite and epidote

Rare albite and epidote are dispersed in the matrix of the micaschists.

The roundish shape of some of the albite crystals suggests that albite could have been formed from no longer present jadeite. Albite is produced from jadeite in the solid-solid net-transfer reaction $NaAlSi_2O_6$ (jadeite) + SiO_2 (quartz) = $NaAlSi_3O_8$ (albite).

Epidote is present only in the garnet-bearing chloritoid micaschists, suggesting that lawsonite could have been previously included in the garnet and then consumed, either during continued prograde growth or during retrograde metamorphism (Winter 2014).

5.2 Estimated peak P-T conditions for the Serre Unit

In addition to the identification of different tectonometamorphic stages from petrographic analysis, peak *P-T* conditions for the Serre Unit can be estimated based on a comparison with peak metamorphic mineral assemblages and corresponding *P-T* conditions of different closely related units from the northern Dora-Maira Massif. The *P-T* conditions of both the Muret Unit and the Chasteiran Unit will be used for this comparison here since they are not only cropping out closely to the Serre Unit but are also consisting mostly of similar rock types (i.e. garnet-chloritoid metapelites). As stated above, the stable mineral assemblage at peak metamorphism (stage 2) observed in the investigated samples from the Serre Unit consists of quartz, white mica, garnet, chloritoid, glaucophane and rutile.

***P-T* pseudosections for the Muret Unit**

The Muret Unit lies directly underneath the Serre Unit in the nappe stack of the northern Dora-Maira Massif. It represents polycyclic basement rocks and consists mainly of garnet-chloritoid micaschists, and minor marbles, metabasites and orthogneisses (Nosenzo et al., 2022).

P-T conditions for the Muret Unit were modelled in pseudosections in the range 10-25 kbar 400-600 °C for three samples of polycyclic micaschists. Two of the samples (GM1, GM2) were collected in a low-strain domain (virtually free from Alpine deformation) and one sample (GM13) was collected in a high-strain domain (pervasive Alpine deformation). The samples are comparable in mineralogical content to those from the Serre Unit. Additionally, GM1 and GM2 contain zoned chloritoid with a zoning pattern similar to the zoned chloritoid described above and GM13 contains accessory graphite. Based on these three samples, metamorphic *peak P-T* conditions for the Muret unit were estimated at 21-22 kbar and 530-560 °C. The pseudosections were calculated considering H_2O in excess, which assumes that the rocks were rehydrated after peak metamorphism (Nosenzo et al., 2023).

The mineral assemblage for the micaschists from the Muret Unit (g-ctd-gl-mu-ru) is identical to the peak mineral assemblage for the Serre Unit. It is located between the garnet-in and chloritoid-in lines but outside the lawsonite-in and chlorite-in lines in all three *P-T* pseudosections (red stars in Fig. 32). The inferred *P–T* path of Alpine garnet growth depicted with grey arrows in pseudosections (b) and (c) marks a transition from a composition which includes lawsonite and chlorite towards the peak mineral assemblage. This inferred *P-T* path is compatible with the suggestion that inclusions of lawsonite in garnet were present in the samples from the Serre Unit but consumed at a later stage.

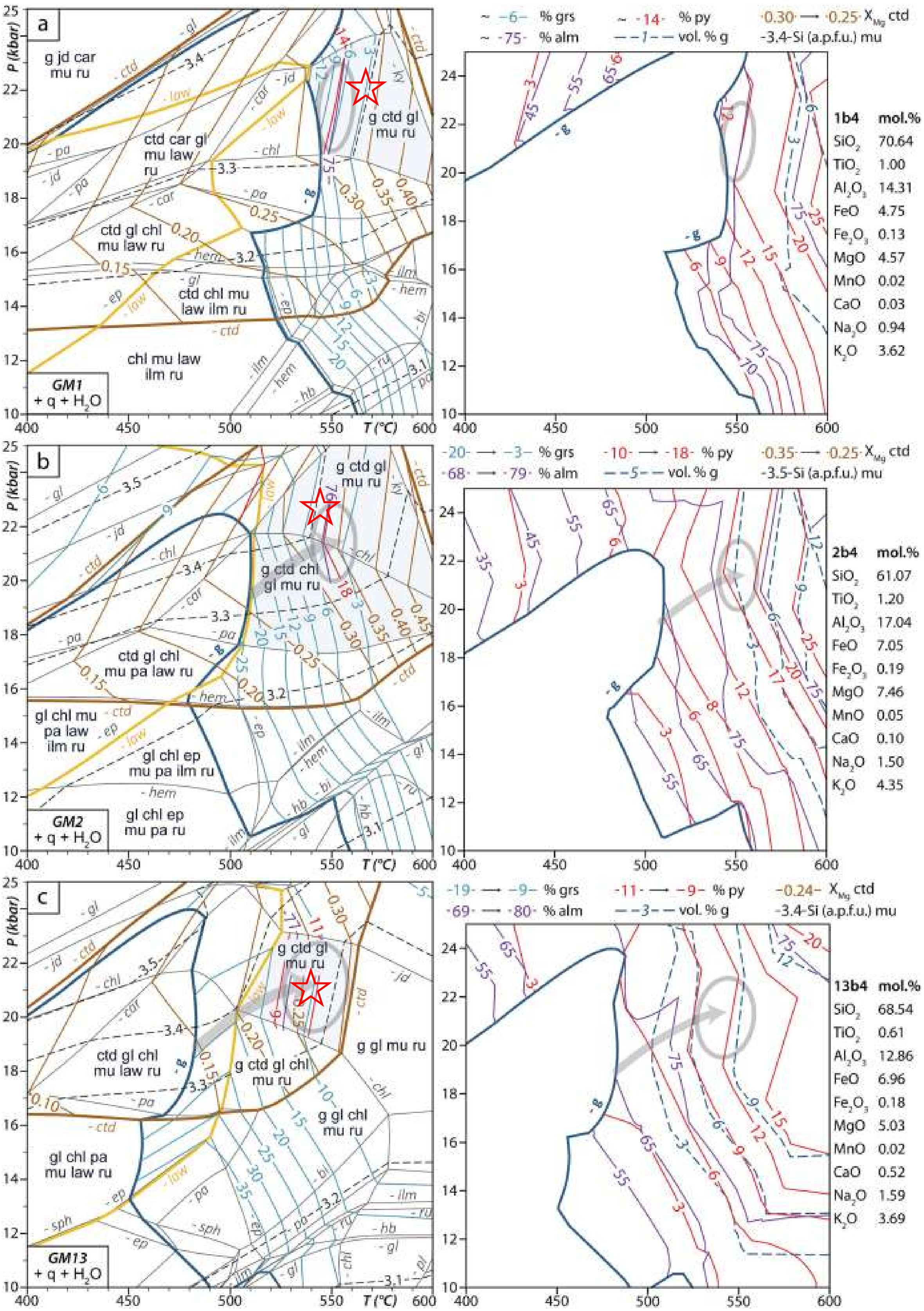

Fig. 32 P–T pseudosections for the Alpine evolution of sample GM1 (a), GM2 (b) and GM13 (c), calculated using H_2O in excess. Some fields are not labelled for the sake of clarity. The garnet-in, chloritoid-in and lawsonite-in lines are depicted in thick blue, brown and yellow lines, respectively. Grey circles indicate the inferred *P–T* conditions of equilibration of $garnet_2$ (sample GM1) and of $garnet_2$ outer portion (samples GM2 and GM13) at peak Alpine stage (stage 1). The grey arrow indicates the inferred *P–T* path of Alpine garnet growth. Estimated P–T conditions for the Serre Unit are indicated by a red star (modified after Nosenzo et al., 2023).

Based on the three *P-T* pseudosections from the Muret Unit, minimum and maximum values for the *P-T* conditions for the Serre Unit can be estimated as:

P-T pseudosections	Min pressure (kbar)	Max pressure (kbar)	Min temperature (°C)	Max temperature (°C)
(a)	18	24	540	600
(b)	19	25	510	600
(c)	18.5	23	500	560
Average	**18.5**	**24**	**517**	**587**

Table 3: Minimum and maximum *P-T* conditions for the mineral assemblage g-ctd-gl-mu-ru in Fig. 32.

The range for peak *P-T* conditions for the Serre Unit therefore lies between 18 and 24 kbar and 520 and 590 °C (rounded values).

Another, different *P–T* pseudosection for the Muret Unit was calculated on the basis of a sample of garnet-chloritoid micaschist (Barkelius 2022). Both the mineral composition and the foliation of this sample are similar to the micaschists from the Serre Unit.

For the mineral assemblage g-ctd-gl-mu-ru, the samples from the Serre Unit plot inside the red line enclosing the fields in which garnet, chloritoid and glaucophane coexist (red star in Fig. 33). Since it was not possible to distinguish between muscovite and paragonite in the optical analysis of the thin sections, the peak mineral assemblage for the Serre Unit could be located both inside and outside the orange line that marks the stability fields for paragonite. As mentioned above, lawsonite and jadeite could have both been present at a previous stage but, even if they were, they are no longer present at peak metamorphism. The location of the peak mineral assemblage for the Serre Unit is therefore further constrained by the lawsonite-in and jadeite-in lines. Talc is absent from the mineral assemblage from the Serre Unit.

Compared with this *P-T* pseudosection for the Muret Unit, the range for peak *P-T* conditions for the Serre Unit can therefore be estimated at 19.5–22.5 kbar and 520–570 °C.

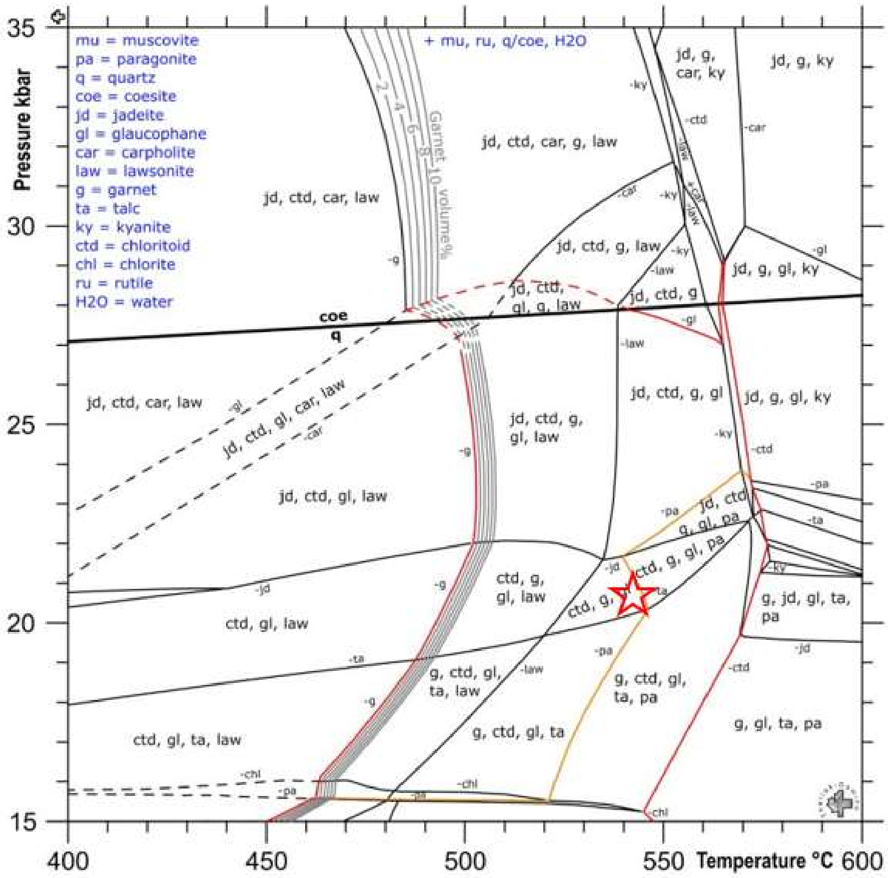

Fig. 33 P–T pseudosection for sample GM1407. In addition to the minerals listed in each field muscovite, rutile, quartz or coesite and water were always present. Small fields are not labelled to avoid clutter. The labels with a minus-sign near the lines show on which side the mineral is unstable. The bold line showing where quartz turns into coesite marks the transition between high-pressure metamorphism below it and ultrahigh-pressure metamorphism above it. The red line encloses all fields were garnet, chloritoid and glaucophane coexist, the orange line encloses the fields that also have paragonite coexisting with muscovite, in addition to the previous minerals mentioned. Estimated P–T conditions for the Serre Unit are indicated by a red star (modified after Barkelius 2022).

P-T pseudosections for the Chasteiran Unit

Another unit situated close to the Serre Unit is the Chasteiran Unit. This unit is located between the Pinerolo Unit and the Muret Unit and was recently identified as an ultrahigh-pressure metamorphism (UHP) unit. Similarly to the Serre Unit, the Chasteiran Unit mainly consists of graphite-rich garnet-chloritoid micaschists with inclusions of chloritoid, rutile and coesite. Polycyclic rocks, such as multistage garnets, were not found there yet. Metamorphic peak *P-T* conditions for this unit have been estimated at 27–28 kbar 510–530 °C (Manzotti et al., 2022).

H_2O saturated *P–T* pseudosections for the Chasteiran Unit were calculated on the basis of a sample of garnet-chloritoid micaschist (CH11). The sample is comparable in mineral composition to the samples from the Serre Unit and also contains similarly zoned chloritoid. However, the garnets in CH11 are optically and chemically zoned into a garnet core and rim and therefore, two different tectonometamorphic stages for garnet growth were identified (Fig. 34).

For the mineral assemblage g-ctd-gl-mu-ru, the location of the *P-T* conditions for the Serre Unit plots to the right of the field for the g-ctd-gl-law assemblage. There is neither lawsonite nor jadeite present at peak metamorphism and the location of the peak mineral assemblage for the Serre Unit is further constrained by the talc-in line (red star in Fig. 34).

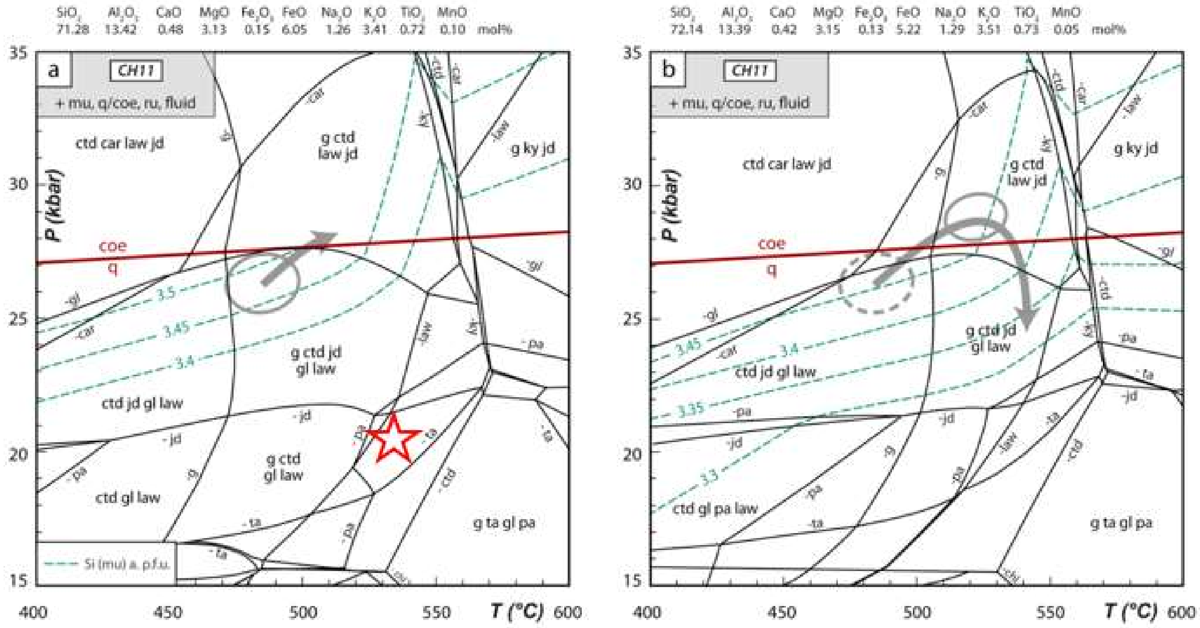

Fig. 34 (**a**) H2O-saturated P–T pseudosections calculated for sample CH11 using the unfractionated bulk-rock composition and (**b**) a composition from which the garnet inner core has been subtracted. Some fields are not labelled for the sake of clarity; their assemblages can be deduced from the assemblages in adjacent fields. Estimated P–T conditions for the samples from the Serre Unit are indicated by a red star (modified after Manzotti et al., 2022).

Comparing the peak mineral assemblage of the Serre Unit with the *P-T* pseudosection for the Chasteiran Unit therefore provides an estimation of peak *P-T* conditions for the Serre Unit at 17.5–22 kbar and 500–565 °C.

To sum up, *P-T* conditions for the peak mineral assemblage for the studied micaschists from the Serre Unit can be estimated by comparing the peak mineral assemblage of the Serre Unit with the *P-T* pseudosections of the Muret Unit and the Chasteiran Unit. *P-T* conditions for the Serre Unit can be estimated as an average value over all the examined *P-T* pseudosections (Table 4). This provides *P-T* conditions at 18-23 kbar and 520-580 °C (values rounded to the nearest tenth).

Study by	Unit	Min pressure (kbar)	Max pressure (kbar)	Min temperature (°C)	Max temperature (°C)
Nosenzo et al., 2023	Muret (a)	18	24	540	600
Nosenzo et al., 2023	Muret (b)	19	25	510	600
Nosenzo et al., 2023	Muret (c)	18.5	23	500	560
Barkelius 2022	Muret	19.5	22.5	520	570
Manzotti et al., 2022	Chasteiran	17.5	22	510	550
	Average	**18.5**	**23.3**	**516**	**576**

Table 4: Average *P-T* conditions for the peak mineral assemblage in the examined *P-T* pseudosections.

Interpretation of *P-T* conditions

A recent study by Westin (2022) examined three samples from the Serre Unit by Raman spectroscopy on carbonaceous material (RSCM). The maximum temperature registered by the studied samples ranged between 480 ± 17 C° and 513 ± 16 °C. These temperatures are lower than the ones estimated here. However, the *P-T* conditions estimated in this thesis are not based on the chemical composition of the minerals. Therefore, it is possible that temperatures are lower. Additionally, paragonite is quite a common mineral in metapelites and is therefore probably present in the samples investigated in this study as well.

The Chasteiran Unit lies between the Pinerolo and the Muret Unit and is thus a little farther away from the Serre Unit within the nappe stack of the northern Dora-Maira Massif. Thermodynamic modelling based on a graphite-rich garnet-chloritoid micaschist from the Chasteiran Unit indicated *P-T* conditions at 27–28 kbar 510–530 °C. These results are consistent with data obtained from the RSCM method which estimated maximum temperature registered by the studied sample at 483 ± 17 °C (Manzotti et al., 2022). Even with the assumption of slightly lower T due to the presence of paragonite, the calculated P for the Chasteiran Unit is still higher than the values obtained by this study. Although the samples from both units are similar regarding mineralogical composition and neither unit contains polycyclic rocks, it is currently assumed that the UHP conditions of the Chasteiran Unit were reached as the unit was detached from the downgoing slab during subduction (Manzotti et al., 2022). In contrast, the Serre Unit consists of rocks that were derived from remnants of a thin Mesozoic cover (Manzotti et al., 2022). A significant difference in the tectonometamorphic history of these two units could therefore explain the incongruence between the *P-T* conditions of these two units.

For the Muret Unit, thermodynamic modelling based on three samples of polycyclic micaschists indicated peak *P-T* conditions at 21–22 kbar and 530–560 °C (Nosenzo et al., 2023) while thermodynamic modelling based on one sample of garnet-chloritoid micaschist indicated peak *P-T* conditions at 22-26 kbar and 510-530 °C (Barkelius 2022). These values, and especially the results obtained by Nosenzo et al. (2023), are more compatible with the values estimated for the Serre Unit in this study and still more so with the assumption of a lower T for the Serre Unit due to the presence of paragonite. Both the similarities of the studied samples regarding mineralogical composition and the very close geographical vicinity of the units add weight to the plausibility of the estimated values for the Serre Unit. Additionally, although the Serre Unit consists of monocyclic rocks while the Muret Unit consists of polycyclic rocks, the *P-T* conditions of the Muret Unit are still comparable to other monocyclic units such as the Pinerolo Unit (Nosenzo et al., 2023). One important difference between the units, however, lies in the Muret Unit consisting of rocks derived from Palaeozoic basement while the Serre Unit features rocks derived from remnants of a thin Mesozoic cover. Therefore, the comparability between the Serre and the Muret Unit notwithstanding, a similar tectonometamorphic history of these two units can still not be assumed without further investigation, and the estimated *P-T* conditions for the Serre Unit must therefore be taken with caution.

5.3 Interpretation of chloritoid zoning

Because zonation records changes in *P-T* conditions during prograde and/or retrograde metamorphism, zoned minerals are particularly useful for deciphering the *P-T* history of a rock (Van der Pluijm 2004). Different factors could have influenced both the distinctive zoning pattern and the total amount of zoning in the chloritoid examined here.

The chloritoid crystals display a distinctive "core-and-margin" type or patchy zoning in which the core of the crystal is rather uniformly coloured until zoning abruptly starts at or near its outer edges (Vernon 2018). There are two main substitutions in chloritoid: Mg and Mn can be substituted by Fe^{2+} and Al^{3+} can be substituted by Fe^{3+} (Nesse 2000). The distinctive zoning pattern that was observed in the examined crystals is constrained by bulk rock composition and especially the content and availability of Mg and Fe during different tectonometamorphic stages. Thus, it could either have been produced by diffusive exchange with the matrix chlorite and ilmenite during cooling of the rock or by a late stage of growth during retrograde cooling or exhumation (Philpotts and Ague 2022).

Support for the latter hypothesis is given in the studies of both the Muret and Chasteiran Unit. In two samples from the Muret Unit, chloritoid crystals with a similar zoning pattern and inclusions of rutile in both the core and the rim were found. The crystals are oriented parallel or at high angle to the pre-Alpine (main) foliation. Chemical analysis indicates a Mg-richer core and a Mg-poorer rim (Nosenzo et al., 2023). Similarly zoned chloritoid crystals with inclusions of rutile in the core and aligned with the main foliation were found in samples from the Chasteiran Unit. Chemical analysis again showed that these crystals contained a Mg-rich core and a Mg-poor, more Fe-rich rim (Manzotti et al., 2022). Both studies suggest that the Mg-rich core of the chloritoid crystals formed at peak metamorphic conditions while the Mg-poor, Fe-rich rim formed at a later stage of growth during retrograde metamorphism.

The optical resemblance between the zoning patterns of the chloritoid from the Serre Unit and those from the Muret and Chasteiran Units suggests that the distinctive zoning pattern of the chloritoid examined here formed in similarly as a result of retrograde growth during Alpine metamorphism.

However, retrograde exchange of Fe and Mg could also have been possible where the choritoid is in contact with chlorite and ilmenite. This could be tested by a future investigation of whether the thickness of the retrograde rim is dependent on the proximity of chlorite and ilmenite with which the chloritoid could have re-equilibrated. Additionally, measuring the mineral compositions of the minerals that are in direct contact with the chloritoid crystals could be used to further constrain the reconstruction of the retrograde history of the rock. Finally, micro-analytical techniques could be used to measure diffusion gradients from the zoned chloritoid crystals. This so-called diffusion chronometry could add valuable information about the timing as well as the speed of the geological processes involved in the zoning of the chloritoid (Philpotts and Ague 2022).

The amount of zoning in chloritoid crystals was examined by measuring the zoned areas visible in the respective thin sections with the help of microphotographs and the software ImageJ. Chloritoid is monoclinic, forming tabular roughly hexagonal or "coffin"-shaped crystals of various thickness parallel to {001} and, like the micas, it has a sheet-like structure consisting of a series of octahedral layers that contain Al^{3+}, Fe^{2+}, Si^{4+}, O and OH (Nesse 2000). This means that any crystal that was not cut parallel to {001} would probably display no or somewhat distorted zoning and measurements could be biased by the way each crystal in the respective thin sections was cut. Consequently, it is important to choose the same crystal faces consistently to facilitate a valid comparison of measurements of the visible amount of zoning.

Recognizing individual crystal faces by optical microscopy alone can be prone to error and is highly dependent on personal experience and skill. Thus, it is possible that some of the crystals considered in this study were not cut properly along a crystal face and therefore represent parts of another crystal. To consistently choose complete crystals with the correct crystallographic orientation, other techniques such as automated electron backscatter diffraction (EBSD) in the scanning electron microscope (SEM) could complement the petrographic analysis in a future study.

The selection of the 15 chloritoid crystals in each thin section could potentially have been further biased towards larger crystals since smaller ones are more readily overlooked or towards “better preserved” crystals in which zonation is more pronounced. These issues of subjective perceptions could be avoided in a future project by first identifying only complete crystals with the same crystal faces and then applying a computer-generated method that randomly selects a certain number of samples.

Finally, although the boundaries between the core and rim areas could mostly be detected by a sharp contrast in colours, the transition was rather gradual in some of the crystals. Therefore, it was not always possible to find the exact demarcation line between the core and the rim and the resulting measurements of the rim may be either too big or too small. However, since the same method for measuring the zoned areas was consistently applied, the same bias should affect all measurements, making them, if not precise, at least comparable.

5.4 Alpine P-T evolution of the Serre Unit

Three different tectonometamorphic stages were identified to characterize the tectonic evolution of the Serre Unit.

Stage 1 is defined unoriented minerals which were preserved as inclusions as both garnet and chloritoid grew. The presence of several inclusions of chloritoid, which is no stable below 14kbar, and rutile in garnet indicates that pressure must have already been higher than 14 kbar at this point. Since the inclusions in garnet and chloritoid don’t display a preferred shape orientation, it is difficult to evaluate the strain history of the samples during this stage.

At stage 2, peak *P-T* conditions were estimated at 18-23 kbar and 520-580 °C. The stable mineral assemblage observed in the investigated samples consists of quartz, white mica, garnet, chloritoid, glaucophane and rutile. The presence of glaucophane at peak metamorphism places the samples from the Serre Unit within the blueschist metamorphic facies and suggests high pressures and low temperatures. These conditions are characteristically developed in subduction zones (Winter 2014). Moreover, the *P-T* conditions estimated for the Serre Unit are comparable to those from the directly underlying Muret Unit while the *P-T* conditions of the Chasteiran Unit, which is still further down in the nappe stack, are significantly higher. This result is compatible with the finding that the units of the northern Dora-Maira Massif display a gradual decrease in temperature from bottom to top (Westin 2022).

Furthermore, stage 2 is associated with the development of the main foliation (S_1) which wraps around the garnets, indicating compression of the foliation around the garnet porphyroblasts. Pressure-shadows occur on one or both sides of the garnets, suggesting that matrix minerals such as white mica were dissolved from high-stress areas and re-precipitated in the low-stress areas adjacent to the crystals in a process known as solution transfer (Winter 2014). Deformation-related microstructures such as mica fish and offset of garnet crystals developed during this stage as well, suggesting deviatoric (shear) stress in addition to normal compressional stress. Microfolding defines the crenulation patterns in S_1 in many of the studied micaschists.

It has been assumed in this thesis that ductile deformation produced both a foliation and the folding of this foliation in a single consistent and progressive event at high *P-T* conditions during this stage. This assumption is supported by the observation that the shape-preferred orientation of chloritoid contributes to the definition of S_1 in all of the micaschist samples while microfolding of chloritoid was recognized in some of the samples as well. Consequently, it is suggested here that the microfolds rather represent local perturbations within the main foliation than indicate separate distinctive deformation events.

Suggesting similar burial mechanisms for the different units of the northern Dora-Maira nappe stack, the strain history of the samples during this stage would be compatible with a model in which the continental crust does not deform continuously during burial. Instead, formation of the main ductile deformation would have been initiated at the beginning of the exhumation history (Manzotti et al., 2022) and associated with the stacking of the different units of the northern Dora-Maira Massif (Nosenzo et al., 2024). In other words, the Mesozoic cover rocks of the Serre Unit could have been subducted together with the whole continental crust during the burial stage while foliation and deformation were probably initiated after peak pressure conditions were reached and stacking of the different units began.

During stage 3, brittle deformation of garnet produces unoriented fractures and suggests decompression at greenschist-facies conditions. Fractures are locally filled by chlorite ± white mica. The main foliation is overgrown by chlorite (which also partly replaces garnet rims), a new generation of chloritoid (identified in the zoned crystals by a darker-blue rim) and ilmenite. Also, replacement of glaucophane occurs during this stage.

Garnet chloritization is more pervasive in samples GM2160A and GM2160B than in samples GM2147, GM1905 and GM2161. This suggests different hypotheses for the tectonic history of these samples. Firstly, the retrograde reactions in these samples could have taken place over a longer period of time during exhumation, indicating that the rock either reached slightly lower *P-T* conditions than the other samples in the first place or was uplifted at a different rate and therefore spent more time in greenschist-facies conditions (Philpotts and Ague 2022). However, this hypothesis is rather improbable because all samples were collected very close to each other. Secondly, exposition to fluids during retrograde metamorphism reverses the continuous dehydration reaction which was used to model the growth of garnet above, resulting in partial replacement of garnet and chloritoid by chlorite. Fluid infiltration can be enhanced by deformation, such as, e.g., in retrograde schist zones, where deformation opens up spaces of low-pressure which suck in fluids and thus promote retrograde reactions (Vernon 2018). The samples displaying more pervasive chloritization could therefore haven been infiltrated by larger amounts of fluid during cooling and/or decompression (Nosenzo et al., 2023). As observed in the samples from the Muret Unit (Nosenzo et al., 2022), exhumation and cooling at greenschist-facies conditions were associated with fluid infiltration, producing chloritization of garnet. Consequently, the pervasive chloritization of garnet in the samples from the Serre Unit could have been produced by similar processes.

To sum up, analysis of the micaschists from the Serre Unit suggests that the Mesozoic cover rocks of the northern Dora-Maira Massif were involved in the Alpine subduction. Increasing temperature and pressure resulted in the development of high-pressure mineral assemblages. Foliation and deformation were probably initiated after peak pressure conditions were reached. Peak *P-T* conditions equivalent to eclogite facies conditions were attained during burial, possibly equivalent to 18-23 kbar and 520-580 °C. This *P-T* evolution is similar to the one experienced by the Muret Unit. This phase was followed by brittle deformation and fluid infiltration at greenschist-facies conditions, which is well documented by the chloritization of garnet, glaucophane and chloritoid as well as pervasive fracturation of garnet.

6. Conclusion

The studied samples from the Serre Unit consist of garnet-chloritoid micaschists, chloritoid micaschists, calcschists and one sample of marble. Investigation of the micaschist samples indicates that the Serre Unit records three distinct tectonometamorphic stages similar to the directly underlying Muret Unit. The first stage is characterized by growth of garnet and chloritoid, as indicated by unoriented inclusions of quartz, white mica, chloritoid, rutile and graphite in both the garnet porphyroblasts and the chloritoid crystals. Stage 2 corresponds to peak *P-T* conditions, estimated at 18-23 kbar and 520-580 °C, on the basis of petrographic observations and comparisons with *P-T* pseudosections calculated for other units of the same nappe stack. The stable mineral assemblage observed in the investigated samples consists of quartz, white mica, garnet, chloritoid, glaucophane and rutile. Finally, stage 3 is characterized by brittle deformation and fluid infiltration at greenschist-facies conditions as indicated by the chloritization of garnet, glaucophane and chloritoid as well as pervasive fracturation of garnet.

This study further confirms the hypothesis that the Mesozoic cover rocks of the Serre Unit were involved in the Alpine subduction. They record a tectonometamorphic evolution similar to the one experienced by the Dora-Maira basement units. The main foliation preserved in the studied samples probably developed after burial at the onset of exhumation. Exhumation and cooling at greenschist-facies conditions was associated with brittle deformation and fluid infiltration.

7. Future work

This study demonstrated that there is great potential in the investigation of the Serre Unit. Future work would include analysis of the chemistry of the main minerals in the samples of garnet-chloritoid and chloritoid micaschist as well as measurement of the bulk rock composition of these samples. Moreover, calculations of *P-T* pseudosections are needed to either confirm or discard the *P-T* conditions of the Serre Unit inferred in this thesis. In fact, the bulk rock composition can greatly influence the stability field of the mineral assemblage since it not only determines the stability of paragonite but also the stability of lawsonite and jadeite at peak metamorphism.

8. Acknowledgments

Special thanks go to my supervisor Paola Manzotti, who made this exciting project possible and supported me throughout the entire process. She was very generous with her time and expertise: always ready to answer questions, give valuable lessons on topics regarding thin sections and mineral identification or provide constructive criticism, advice and motivation. I would also like to thank Robert Dunst and Alexandre Jean Daniel Peillod for helping with the practical challenges of working with thin sections, and my husband, Urs Wehrli, for his unconditional love and encouragement.

9. References

Bachmann, R., Glodny, J., Oncken, O., Seifert, W., 2009: Abandonment of the South Penninic–Austroalpine palaeosubduction zone, Central Alps, and shift from subduction erosion to accretion: constraints from Rb/Sr geochronology. *Journal of the Geological Society*, *166*(2), 217-231.

Ballèvre, M., Camonin, A., Manzotti, P., Poujol, M., 2020: A step towards unravelling the paleogeographic attribution of pre-Mesozoic basement complexes in the Western Alps based on U-Pb geochronology of Permian magmatism. *Swiss Journal of Geosciences* 113(1).

Barkelius, M., 2022: Garnet-chloritoid micaschist as a Key to Decipher the Metamorphic Evolution of the Continental Crust: A Case Study from the Dora-Maira Massif (Western Alps). Bachelor thesis in Geoscience, University of Stockholm.

Bonnet, G., Chopin, C., Locatelli, M., Kylander-Clark, A. R. C., Hacker, B. R., 2022: Protracted subduction of the European hyperextended margin revealed by rutile U-Pb geochronology across the Dora-Maira massif (W. Alps). *Tectonics 41*.

Chopin, C., 1984: Coesite and pure pyrope in high-grade blueschists of the Western Alps: a first record and some consequences. *Contributions to Mineralogy and Petrology*, 86(2):107–118.

Franceschelli, M., Memmi, I., 1999: Zoning of chloritoid from kyanite-facies metapsammites, Alpi Apuane, Italy. *Mineralogical Magazine* 63(1), 105-110.

Frost, B. R., Frost, C. D., 2019: *Essentials of Igneous and Metamorphic Petrology*. 2nd ed. Cambridge: Cambridge University Press.

Groppo, C., Ferrando, S., Gilio, M., Botta, S., Nosenzo, F., Balestro, G., Festa, A., Rolfo, F., 2019: What's in the sandwich? New P-T constraints for the (U)HP nappe stack of southern Dora-Maira Massif (Western Alps). *European Journal of Mineralogy* 31(4): 665–683.

Holland, T. J. B., Powell, R., 2011: An improved and extended internally consistent thermodynamic dataset for phases of petrological interest, involving a new equation of state for solids. *Journal of Metamorphic Geology*. 29(3):333–383.

Lindsley, D., 1991: *Oxide Minerals: Petrologic and Magnetic Significance*. Berlin, Boston: De Gruyter.

Liou, J.G., Zhang, R.Y., Ernst, W.G., Rumble, D., Maruyama, S., 1998. High pressure minerals from deeply subducted metamorphic rocks. In: *Ultrahigh-Pressure Mineralogy: Physics and Chemistry of the Earth's Deep Interior*. Chantilly, Virginia: Mineralogical Society of America.

Manzotti, P., Ballèvre, M., Zucali, M., Robyr, M., Engi, M., 2014: The tectonometamorphic evolution of the Sesia–Dent Blanche nappes (internal Western Alps): review and synthesis. *Swiss Journal of Geosciences* 107(2–3): 309–336.

Manzotti, P., Pitra, P., Langlade, J., Ballèvre, M., 2015: Constraining P-T conditions during thrusting of a higher pressure unit over a lower pressure one (Gran Paradiso, Western Alps). *Journal of Metamorphic Geology* 33(9): 981–1002.

Manzotti, P., Ballèvre, M., Poujol, M., 2016: Detrital zircon geochronology in the Dora-Maira and Zone Houillère: a record of sediment travel paths in the Carboniferous. *Terra Nova* 28(4): 279–288.

Manzotti, P., Bosse, V., Pitra, P., Robyr, M., Schiavi, F., Ballèvre, M., 2018: Exhumation rates in the Gran Paradiso Massif (Western Alps) constrained by in situ U–Th–Pb dating of accessory phases (monazite, allanite and xenotime). *Contributions to Mineralogy and Petrology* 173(3).

Manzotti, P., Ballèvre, M., Pitra, P., Schiavi, F., 2021: Missing lawsonite and aragonite found: P-T and fluid composition in meta-marls from the Combin Zone (Western Alps). *Contributions to Mineralogy and Petrology* 176, 60.

Manzotti, P., Schiavi, F., Nosenzo, F., Pitra, P., Ballèvre, M., 2022: A journey towards the forbidden zone: a new, cold, *UHP* unit in the Dora-Maira Massif (Western Alps). *Contributions to Mineralogy and Petrology* 177(6).

Meinhold, G., 2010: Rutile and its applications in earth sciences. *Earth-Science Reviews,* 102(1–2). 1-28.

Miyashiro, A., 1994: *Metamorphic Petrology*. London: UCL Press.

Nesse, W. D., 2000: *Introduction to Mineralogy*. 3rd ed, New York: Oxford University Press.

Nosenzo, F., Manzotti, P., Poujol, M., Ballèvre, M., Langlade, M., 2022: A window into an older orogenic cycle: P–T conditions and timing of the pre-Alpine history of the Dora-Maira Massif (Western Alps). *Journal of Metamorphic Geology* 40(4): 789–821.

Nosenzo, F., Manzotti, P., Krona, M., Ballèvre, M., Poujol, M., 2024: Tectonic architecture of the northern Dora-Maira Massif (Western Alps, Italy): field and geochronological data. *Swiss Journal of Geosciences* 117(1).

Nosenzo, F., Manzotti, P., Robyr, M., 2023: H2O budget and metamorphic re-equilibration in polycyclic rocks as recorded by garnet textures and chemistry. *LITHOS* 452-453.

Pereira, I., Craig, D. S., 2023: Detrital rutile: Records of the deep crust, ores and fluids. *LITHOS* 438-439.

Pfiffner, O. A., 2014: *Geology of the Alps*. Revised and updated translation of Geologie der Alpen. 2nd ed., John Wiley & Sons.

Philpotts, A. R., Ague, J. J., 2022: *Principles of Igneous and Metamorphic Petrology*. 3rd ed. Cambridge: Cambridge University Press.

Rasband, W. S., 1997-2018. ImageJ, U. S. National Institutes of Health, Bethesda, Maryland, USA, https://imagej.net/ij/.

Schmid, S. M., Kissling, E., 2000: The arc of the western Alps in the light of geophysical data on deep crustal structure. *Tectonics*, *19*, 62–85.

Schmid, S. M., Fügenschuh, B., Kissling, E., Schuster, R., 2004: Tectonic map and overall architecture of the Alpine orogen. *Eclogae Geologicae Helvetiae* 97(1): 93-117.

Tajčmanová, L., Manzotti, P., Alvaro, M., 2021: Under pressure: high-pressure metamorphism in the Alps. *Elements: An International Magazine of Mineralogy, Geochemistry, and Petrology*, *17*(1), 17-22.

Van der Pluijm, B. A., Marshak, S., 2004: *Earth structure: an introduction to structural geology and tectonics*. 2nd ed., New York: W.W. Norton.

Vernon, R. H., 2018: *A Practical Guide to Rock Microstructure*. 2^{nd} ed., Cambridge: Cambridge University Press.

Westin, W., 2022: Thermal structure of a paleo-subduction zone (Dora-Maira Massif, Western Alps). Master thesis in Geology, Stockholm University.

Winter, J. D., 2014**:** *Principles of Igneous and Metamorphic Petrology*. 2^{nd} ed. Essex: Pearson.

Yardley, B. W. D., MacKenzie, W. S., Guildford, C., 1990: *Atlas of metamorphic rocks and their textures*. Burnt Hill, Harlow, Essex, England: Longman Scientific & Technical; New York, NY: Wiley.

Yardley, B., Warren, C., 2021: *An Introduction to Metamorphic Petrology*. 2^{nd} ed., Cambridge: Cambridge University Press.